NEURONAL GROWTH PATTERNS IN STATES OF LEARNING AND ACTIVITY BLOCKADE

by

Serhiy Opushnyev

B.Sc. (Hons), The University of British Columbia, 2013

A THESIS SUBMITTED IN PARTIAL FULFILLMENT OF

THE REQUIREMENTS FOR THE DEFREE OF

MASTER OF SCIENCE

in

THE FACULTY OF GRADUATE AND POSTDOCTORAL STUDIES

(Neuroscience)

THE UNIVERSITY OF BRITISH COLUMBIA

(Vancouver)

March 2017

Abstract

The role of activity on the formation of neural networks during development is known to be critical. In the research conducted for this dissertation the effect of experience was probed at the single neuron level. First, a method for selecting neurons based on their responses to a visual stimulus and electroporating the selected neurons in a somata dense region was developed. This method was then used to select neurons responsive to a predetermined visual stimulus and the growth behavior of the neuronal arbor was observed in the presence of visual stimuli. When neurons were trained to better discern the visual stimulus the plasticity of the neuron was correlated with the dendritic growth behavior. In general, responsive neurons tended to prune their dendritic arbors while non-responsive neurons tended to grow. Interestingly, neurons that acquired a response with training tended to grow before acquiring a response and prune after. Blockade of NMDA receptors abolished these effects. In a separate set of experiments dendritic growth patterns were observed while all excitatory activity was blocked pharmacologically. These experiments showed that short-term (1.5 hours) excitatory activity blockade does not alter dendritic growth patterns. However, 30 minutes after the start of the activity blockade, the density of filopodia increased, suggesting that the neuron was compensating for the lack of activity.

Preface

Chapter 2:

I designed and performed all experiments and prepared the figures.

Chapter 3:

K. Podgorski and I contributed equally to this work. I designed and performed imaging experiments, processed raw data and performed analysis. Kaspar Podgorski designed and performed imaging experiments, processed raw data, performed analysis and prepared the figures. Prof. K. Haas provided advice on experimental design.

Chapter 4:

I designed and performed experiments, processed raw data, performed analyses and prepared the figures. Sina Safa and Jodi Wong assisted in performing experiments (3 data points) and processing data (3 data points). Prof. K. Haas provided advice on experimental design.

All studies were performed with the approval of the UBC Animal Care Committee (certificates: A09-0021 and A15-0279)

Table of Contents

List of Tables

List of Figures

Acknowledgements

First of all I would like to thank my supervisor Dr. Kurt Haas for giving me the freedom to mature by exploring my ideas and interests. Without your guidance and support I would not be the person I am now. I would also like to thank my supervisory committee, Dr. Catherine Rankin and Dr. Tim O'Connor, for your patience and advice.

Thank you also to my colleagues in the Haas lab. Specifically I would like to thank Kaspar Podgorski, Janaina Brusco, Kathryn Post, Dong Hwan Kim, Kelly Sakaki and Lara Thompson. I would also like to thank all the students that helped me with my experiments – Jodi Wong, Sina Safa and Nicole Cheung.

A special thanks to my family for their unwavering support and encouragement.

Chapter 1: General Introduction

During early brain development neurons undergo extensive morphological growth and plasticity. Neurons extend large axonal and dendritic arbors while establishing a multitude of synaptic connections, which facilitate the integration of the neuron into functional circuits. Since neuronal morphology can impact neural processing, abnormal structural growth, or incorrect connectivity in the brain, can contribute to a range of neurological and neurodevelopmental disorders such as schizophrenia, Down's syndrome, fragile X syndrome, Angelman's syndrome, Rett's syndrome and Autism Spectrum Disorder (ASD)[1–8]. Thus, understanding how a neuron grows and integrates into brain networks is critical for understanding the underlying cause of neurodevelopmental disorders, and is the first step toward creating a preventative treatment or cure.

Direct imaging of brain neuron dendritic arbor growth in intact developing brains reveals a multiphasic process[9–11]. Neurons are first formed as simple spheres without processes, and then progress through three phases. In the first phase, neurons extend an axon to the target region and dendrite growth is restricted to the extension and high turnover of short filopodia, characterized as highly motile actin rich processes typically less than 10um in length. It has been proposed that during this stage, axonogenesis dominates as the axon navigates to its target and establishes a terminal arbor. In the second phase of dendritogenesis, dendritic filopodia can elongate and transition into longer and more stable branches allowing for a dramatic burst of growth and rapid establishment of the dendritic arbor. During this phase the dendritic arbor is highly motile. Both filopodia and dendritic branches are constantly being formed and eliminated. Finally, in the third phase of dendritogenesis, the dendritic arbor becomes stabilized with little net change in total branch length or number, and addition, motility, and turnover of filopodia are reduced. This progression of development was observed *in vivo* in *Xenopus laevis* tadpoles[9,10]. In contrast to the

developmental progression described above, studies conducted *in vitro* describe the initial stages of the developmental progression differently. In culture, neurons first extend a number of neurites, which are believed to be undifferentiated progenitors of both dendrites and axons. Typically, the longest neurite then differentiates to adopt an axonal fate, and the rest differentiate into dendrites[12–15]. The difference between the *in vivo* and *in vitro* developmental progression, namely the initial extension of neurites *in vitro*, may be a consequence of cultured neurons not receiving the requisite cues from their environment to determine where the axon will need to grow before neurites extend.

A neuron is a highly polar cell that is composed of three major compartments, the dendritic arbor, the soma, and the axonal arbor. Each compartment has a role to play in signal propagation, specifically, the dendritic arbor is where the majority of synaptic input from upstream neurons is received and integrated, the soma is where the summation and integration of synaptic input determines whether an 'all-or-none' action potential (AP) is triggered, and the axon serves to transmit the AP from the soma to distant downstream targets. The flow of information is thus as follows: in an upstream presynaptic neuron an AP is generated at the axon hillock and travels down the axon to the pre-synaptic terminal to initiate neurotransmitter release. The released neurotransmitters cross the synaptic cleft and binds to post-synaptic receptors generating an excitatory post-synaptic potential (EPSC). EPSCs from multiple synapses are then integrated in the dendritic arbor and soma of the downstream neuron and may contribute to the generation of another action potential.

Therefore, dendritic and axonal arbors have differing functions. Dendrites function to receive and integrate neural information encoded in synaptic activity[16–18]. Once this information is integrated it is transformed and encoded in action potential firing which is propagated to downstream neurons via axons. The functional differences are also evident from the structure of these compartments.

Dendritic arbors extend locally from the soma, while axonal processes can project long distances before terminating in arbors in target regions. Despite targeting differences between these structures, the processes underlying terminal axonal and dendritic arbor formation are similar. On a cytoskeletal level, both dendritic and axonal arbors are composed of microtubules and actin. However, the microtubules in axons have a plus-end distal orientation while microtubules in dendrites have a mixed orientation[19,20]. At the level of organelles, dendrites contain Golgi outposts while axons do not[21]. At the molecular level, axons and dendrites contain different microtubule binding proteins: tau in axons, and MAP2 and CHO1/MKLP1 in dendrites[22,23]. Similarly, GAP43 is found in axons and their growth cones but is absent from dendrites[24].

1.1 Historical progression of investigations into dendritogenesis

The investigation into how dendritogenesis occurs began over a century ago at the time of Golgi and Cajal. Techniques like the Golgi stain, which is a silver stain that selectively darkly stains the full morphologies of a small fraction of neurons within intact tissues, allowed for the first time, visualization of neuronal structures. Neuronal morphological development was studied by observing fixed brain tissues at different developmental stages[25]. These initial investigations concluded that dendritogenesis is a continuous process of branch elongation and bifurcation. More recently, low-density cultures were used to study dendritogenesis[12–14]. From these experiments it was observed that dendritogenesis is a much more dynamic process than was previously thought, involving the continuous extension and retraction of both smaller structures and long branches. Current work examining dendritogenesis employs direct imaging within the intact brains of developing animals[9,10,26–30]. The majority of these studies involve *in vivo* studies in embryos of *Xenopus laevis* and zebrafish using florescent indicators expressed in individual brain neurons together with rapid time-lapse imaging on a time scale ranging from minutes to days[9,10,26–28]. These

studies concluded that growth cones at the tips of dendritic branches mediate both elongation and bifurcation. Furthermore, dendritic filopodia, short and thin actin-rich protrusions from dendrites, were observed to be able to transform into nascent branches[9,10,29]. During dendritogenesis filopodia exhibit high rates of turnover with the majority of filopodia being eliminated within minutes of extension[9–11]. A small fraction of dendritic filopodia stabilize and grow into longer and more stable branches[9–11].

1.2 Dendritic patterning is critical for signal processing

Dendrites take on an array of shapes from the highly complex dendritic arbors of the cerebellar Purkinje neurons to the relatively simple hippocampal dentate gyrus granule cells. The precise branching pattern of any neuron determines how signals from synapses are integrated (for review see [18]). To understand how the branching pattern influences signal integration I will briefly review some theories about signal propagation through dendrites. Early simple cable models assume dendrites act as passive wires through which signal strength decays as a function of length and diameter[31]. Thus, the distance from the synapse to the soma alone is a critical contributor to how much influence a synaptic input contributes to somatic firing[32–34]. Later theories modelled dendrites as active cables, which retain the passive properties but also incorporate regenerative events similar to action potentials in axons (for a review see [35]). The regenerative dendritic potentials can also arise from non-linear summation of multiple excitatory post-synaptic currents (EPSCs)[36–38]. The spatial organization of synapses and branch points influences the degree of nonlinear summation, since nearby synapses are more likely to interact, and branch points can both hinder transmission, or regenerate signals by voltage-gated calcium channels. Therefore, the precise patterning and shape of dendritic arbors and distribution of synapses determines how signals are integrated and contribute to action potential firing.

1.3 Mechanisms of dendritic arbor patterning: synaptotropic hypothesis

A major question of developmental neuroscience is: *How do brain neurons achieve their dendritic arbor patterning and distribution of synaptic inputs?* One clear answer is that genetic programs dictate general arbor shape for neurons within each type or class. Brain neurons are largely classified based on dendritic arbor morphology since neurons within the same group share overall structure. Moreover, neurons grown in dissociated culture often retain basic morphologies seen *in vivo*[12–14]. However, each neuron within a group is unique in the precise location and number of branches, suggesting that patterning is not completely hardwired by genetic programs. A number of studies support a model in which the fine dendritic arbor patterning is influenced by neural activity (for review see [27]).

These findings have led to further questions on the molecular mechanisms mediating activity-dependent dendritogenesis. A leading model is the synaptotropic hypothesis, which was proposed based on early work by Vaughn on synaptogenesis and dendritic arborization in fixed rat spinal tissue[39–41]. It was observed that the dendrites of motor neurons predominantly grew into the regions of developing mouse spinal cord that were enriched with afferents and synapses. Vaughn hypothesized that synapses have a local stabilizing effect on the dendritic tree. Since these initial observations many studies have supported and elaborated upon this model (for a review see [42]).

Many of the details for the synaptotropic hypothesis were derived from *in vivo* time-lapse imaging studies in *Xenopus laevis* tadpoles and larval zebrafish. The transparency of both of these model systems offer direct visualization of growth of individually-labelled brain neurons within intact animals. Time-lapse imaging studies in zebrafish tectal neurons revealed that dendritogenesis and synaptogenesis are concurrent[29]. Furthermore, time-lapse data sets of growing neurons demonstrated that dendritic filopodia are highly motile structures that are continuously added and

eliminated from dendritic branches[10,28,29]. Experiments imaging both filopodial motility and a fluorescent marker of excitatory synapses (PSD95-GFP) found that filopodia with PSD95 puncta, and presumably excitatory synapses, became stabilized[29]. In a seminal study by Chris Neill and Stephen Smith, they found that when dendritic filopodia first extend from existing dendrites they are highly motile, lack synapses, and often retract into the dendrite[29]. In some cases, filopodia develop PSD95 puncta, which is correlated with decreased filopodial motility and increased lifetime. Neill and Smith observed that filopodia with PSD95 puncta could still demonstrate extension and retraction, but this was limited to portions distal to the puncta. They also found that new filopodia often extended from sites of PSD95 puncta. Furthermore, these filopodia only fully retracted if the PSD95 puncta first disappeared. In a careful later study by Hossain, in which filopodia were tracked over long periods, it was observed that stabilized filopodia can further elongate and transition into branches[10]. Typically, filopodia are classified as highly motile, actin rich processes shorter than 5-10 microns, while branches are longer and are stabilized by microtubules. These findings support a role for synapse formation in stabilizing filopodia, supporting their transition into longer branches, and providing sites for new process extension. Thus, the synaptotropic model suggests that dendritic arbors grow iteratively, building on synaptic stabilization points. An important implication of this model is that if synapses direct dendritic patterning, and if neural transmission influences synaptogenesis, then activity-directed growth allows for the self-organization of neuronal morphology resulting in structures optimized to encode the activity encountered during development.

One limitation of the original synaptotropic hypothesis proposed by Vaughn is that it did not explain why dendritic arbors stop growing at the end of the critical period of dendritogenesis. To address this, an expanded, modified version of the synaptotropic hypothesis was proposed in which

graded levels of synaptic strength confer graded levels of morphological stabilization[43]. A simple interpretation of the synaptotropic model of dendritogenesis would be that manipulations which increase synapse formation and strength would promote arbor growth and complexity, while manipulations that weaken synapses would stunt growth. Evidence supporting a graded model of synaptotropic growth comes from *in vivo* time-lapse imaging of *Xenopus laevis* tectal neurons in which synaptic strength is increased or decreased. Over-expression of plasticity promoting proteins, including CaMKII, Homer 1b, and PKM$_\zeta$, which drive synaptic maturation, resulted in a reduction in dendritic arbor elaboration[44–46]. Interestingly, strengthening glutamatergic synapses decreased filopodial motility and turnover, producing hyper-stabilized arbors. Manipulations that decreased synaptic strength, including inhibitory peptides blocking AMPA receptor insertion into synapses or PKM$_\zeta$ resulted in destabilized filopodia, exhibiting increased motility and turnover[30,46]. Since filopodia on these neurons failed to stabilize and transition into branches, their overall arbor complexity was also decreased. Other work looked at other components of synaptic transmission, specifically calcium influx. Calcium influx is sufficient to induce filopodial stabilization[44,47–49]. Conversely, pharmacologically reducing calcium events led to growth of filopodia and filopodia sprouting from dendritic branches[48].

Evidence against the synaptotropic hypothesis also exists. One study looking at brain development in mice observed that munc-18, a protein essential for neurotransmitter release, knock-out mice had structurally normal looking brains, suggesting that activity across a synapse is not essential for brain development[50]. However, this study did not examine morphology of dendritic arbors, the functional properties of synapses or neural encoding. It is possible that without synaptic transmission, other mechanisms drive synaptogenesis, such as cell adhesion signaling[51], and that while the brain looks normal brain circuits are not functional. In support of this idea, the authors

remarked that after the correct assembly of the brain, neurons began to undergo apoptosis. Interestingly, apoptosis began earlier in brain areas that develop sooner and was seen before birth, which is fatal in this mutant, suggesting that it was a property of the connectivity that caused the neurodegeneration rather than a physiological cause such as absence of breathing.

1.4 Synaptogenesis

Experiments supporting the synaptotropic hypothesis show that synaptogenesis is a critical part of dendritogenesis. Synaptogenesis is comprised of multiple distinct steps. Initially, a complex assortment of cell adhesion molecules (CAMs), including distinct proteins and their splice variants on axonal and dendritic membranes[52], interact and confer 'synapse specificity' by identifying correct partners to form initial axo-dendritic contacts based on pre- and postsynaptic CAM binding affinity[53–55]. Compatible interactions produce trans-neuronal binding and clustering of additional CAMs on each cell through 'cis-interactions' due to CAM-CAM dimerization. The enlarged trans-neuronal structural contact sites are called adhesion junctions, which serve to physically keep the two membranes near each other and mediate clustering of intracellular synaptic components. Evidence that CAMs are sufficient for initiation of synapse formation comes from experiments expressing CAMs in non-neuronal cells which are co-cultured with neurons. For example, HEK293 cells expressing the postsynaptic CAM Neuroligin co-cultured with neurons induced formation of presynaptic structures where axons made contact with the non-neuronal cells[56]. CAMs attract and cluster pre- and post-synaptic intracellular protein complexes by PDZ protein binding sites in their intracellular domains[55,57,58]. By linking to scaffolding proteins, such as PSD95, which in turn link to cytoskeletal binding proteins, CAMs can both stabilize nascent synapses and the cytoskeleton[51,55]. At presynaptic sites, CAMs induce clustering of neurotransmitter vesicles and machinery for vesicle release and recovery[59]. On the postsynaptic

side, CAMs can induce clustering of NMDA receptors (NMDARs)[59]. Once the nascent synapse is formed, rudimentary presynaptic neurotransmitter release can activate postsynaptic NMDARs, which has been shown to be critical for subsequent synapse maturation. NMDAR activation allows calcium entry, which triggers 'AMPA-fication' or the insertion of AMPA receptors (AMPARs) in to the synapses[60–62]. Further synapse maturation ensues, involving shifts in receptor and NMDAR and AMPAR subunit expression[62–64].

1.5 Brief overview of plasticity

Once a synapse is established and matured, it can undergo further changes to its strength, or the size or efficiency of the propagation of its signals. Changes in synaptic strength can be driven by patterns of synaptic transmission and are referred to as 'synaptic plasticity'. An activity-dependent increase in synaptic strength is termed 'long-term potentiation (LTP)', and decreases in strength are 'long-term depression (LTD)'. The elucidation of the molecular pathways that are activated by LTP and LTD inducing stimuli that shift synaptic strength have been a major focus of the field of neuroscience since LTP was first experimentally demonstrated in 1973[65]. While a number of pre- and post-synaptic mechanisms have been identified in a wide range of synapses, in most models, LTP and LTD are produced by an increase and decrease in the number of AMPARs in the synapse, respectively (for a review see [66]). While synaptic plasticity is typically studied in mature brain circuits, the developing brain exhibits the height of synaptogenesis and synaptic plasticity which is intricately involved with dendritic arbor formation through synaptotropic dendritogenesis mechanisms[29]. In our graded synaptotropic model, nascent synapses undergoing activity-dependent LTP strengthens the underlying cytoskeleton and region of dendrites, while LTD leads to destabilization, and potential synapse and process loss.

1.6 Intrinsic versus extrinsic factors directing dendritic arbor patterning

While classification schemes vary widely, early attempts based on dendritic morphology identify more than 5,000 distinct types of neurons. Importantly, while individual neurons within a type had a very stereotypical general dendritic arbor patterning common to the group, the fine details between individual neurons, such as branch placement and number were unique[67]. Moreover, when cultured, neurons of recapitulated basic aspects of their stereotypical shapes despite the absence of the normal environmental cues[12–14]. Altogether, this data supports a model in which dendritic arbor patterning is a combination of intrinsic genetic programs that lay down basic structures, and extrinsic factors that influence the fine-tuning of the higher order structures.

Little is known of how genes control dendritic arbor patterning. The most advanced investigations have made use of mutation screens in the fruit fly *Drosophila melanogaster*. Critically, in *Drosophila* it is possible to identify the same neuron across individuals, such as 'dendritic arborization (DA) neurons'. DA neurons are subdivided into four classes (I, II, III, and IV) in order of increasing dendritic arbor complexity[68]. Using mutation screens, the Jan lab has determined that the general dendritic arbor patterning of DA neurons is determined by the levels of expression of the transcription factors *abrupt, cut* and *spineless*[69–72]. *Abrupt* expression is normally limited to class I DA neurons. When *abrupt* is ectopically expressed in neurons of the other DA classes, reduced branch numbers occur[71,72]. *Cut* is expressed in class II, III and IV DA neurons at low, high and intermediate levels, respectively. When expression of *cut* is eliminated in class III or IV DA neurons, their dendritic arbors resemble those of DA class I and II neurons[70]. In general, dendritic growth and terminal branching is lost without the expression of *cut*. Unlike *cut* and *abrupt*, *spineless* is expressed in all four DA neuronal classes but it has class-specific effects. In class I and II DA neurons *spineless* reduces branch complexity while it increases branch complexity in

class III and IV DA neurons[73]. Thus the expression levels of *abrupt*, *cut*, and *spineless* govern the class to which a DA neuron will belong. In a similar vein, the transcription factor *hamlet* can convert a highly complex, highly branched multi-dendritic neuron into ones expressing a simple dendritic arbor, similar to an external sensory neuron[74]. The profound effect of transcription factors on neuronal morphology can be observed in other model organisms as well. For example, knock-out of the transcription factor CREST in mouse leads to less elaborate basal and apical dendrites of pyramidal neurons in hippocampus and cortex[75]. Similarly, the transcription factor Neurogenin2 promotes outgrowth of a polarized leading process in pyramidal neurons in rat neocortex[76].

A larger body of research has identified extrinsic factors that influence the fine structure and orientation of dendritic arbor patterning. A number of categories of extrinsic stimuli have emerged, including guidance cues, neurotrophic factors, excitatory glutamatergic synaptic transmission and neuronal firing. The term 'guidance cues' traditionally refers to proteins found to guide axonal growth acting as either chemo-attractants or -repellents to dynamic axonal growth cones. Gradients of guidance cues direct axonal growth cone navigation for precise pathfinding to target regions where axons form terminal arborizations.

While a vast literature focuses on axonal growth cones and their regulation by guidance cues[77,78], few studies have examined dendritic growth cones and their potentially similar abilities to detect and navigate external guidance cues[79]. Some of the traditional axonal guidance cues have been found to influence dendritic growth, including Sema3A and slit. In the rodent cortex Sema3A has been shown to act as a chemoattractant for dendrites, orienting pyramidal neuron apical dendrites toward the pial surface, while simultaneously repelling axons to establish neural polarity[80]. Alternatively, the axonal guidance cue slit has been shown to increase dendritic branching without affecting dendritic orientation in some cases[81,82] while in others slit mediated dendritic guidance[83].

The neurotrophic factors are a family of molecules that induce growth and survival of immature neurons and play a role in neuronal survival and regrowth following injury. The main neurotrophic factors implicated in dendritogenesis are nerve growth factor (NGF), brain derived neurotrophic factor (BDNF), neurotrophic factor 3 (NT-3) and neurotrophic factor 4 (NT-4). All of these factors affect cells by binding to their receptors, TrkA, TrkB, TrkC and TrkB, respectively, expressed on the surface of the cell. For example, systemic application of NGF on developing rat sympathetic ganglion neurons for 1-2 weeks resulted in increased dendritic branching and increased total dendritic branch length (TDBL)[84,85]. Conversely, treatment of the same preparation with NGF antiserum decreased TDBL. In rat cortex, the effects of neurotrophins have been found to be layer and dendrite type specific. In layer 4 pyramidal neurons, basal dendrites respond strongly only to BDNF, while basal dendrites of layer 5/6 pyramidal neurons respond strongly to NT-4, and their apical dendrites respond strongly to several neurotrophins[86]. NT-3 was potent in promoting dendritic growth of pyramidal neurons while non-pyramidal neurons showed no dendritic responses[87]. Evidence demonstrates that the source of neurotrophins and the cellular compartment expressing specific receptors, determines their disparate effects. For example, retinal ganglion cells (RGCs) in *Xenopus* are exposed to two sources of BDNF, each of which has a unique effect on RGC dendritogenesis. BDNF secreted by nearby retinal neurons restricts local RGC dendritic branching, while BDNF secreted by downstream postsynaptic targets in tectum stimulates dendrite growth in upstream RGCs[88,89].

One of the most salient external stimuli for an organism is sensory activity. This is the information that an animal uses to effectively navigate its environment throughout life. Evidence for the idea that sensory stimuli are important for brain development came from findings that visual cortical pyramidal neurons had more complex arbors when animals were reared in stimulation rich

12

environments compared to those reared in stimulus-sparse environments[90,91]. Other evidence came from studies that modified sensory stimulation more directly. Modifying the sensory stimuli, or the pattern of stimuli, that an animal perceives is a powerful method to study how circuits during development and maturity adapt to the incoming information. A number of methods have been used to non-invasively modify the sensory stimuli that an animal interacts with. Many of these methods rely on removing sensory input. Suturing either one or two of the eyelids of kittens is one example[92–94]. In their studies Hubel and Weisel found that visual deprivation has a profound effect during a critical period in development, the first 3 months of life for cats and the first 6 months for primates, but not after[95,96]. Suturing one eyelid for the duration of the critical period resulted in the ocular dominance columns for the deprived eye becoming smaller and those for the open eye increasing in size. Furthermore, they observed that in the visual cortex, the number of layer 2/3 pyramidal neurons that responded to stimuli from both eyes decreased dramatically when one eye was deprived of activity. Interestingly, when both eyes were sutured shut, the visual cortex neuronal responsiveness retained a response distribution of the two eyes that mirrored normal animals, although responses were weaker. Experiments examining effects on neuronal morphology found that monocular deprivation in kittens led to the atrophy of dendritic arbors of cortical layer 4 pyramidal neurons innervated by the deprived eye in the LGN[92]. Similar results were found in deprivation experiments in other sensory modalities. Unilateral ear plugging disrupted the symmetric development of dendritic arbors of nucleus laminaris neurons which receive binaural innervation[97]. In somatosensory barrel cortex of mice, where sensory input from whiskers is neatly organized into barrels of neurons, whisker trimming was found to markedly reduce dendritic arbor protrusive motility in the deprived regions of barrel cortex[98].

Interestingly, when sensory stimuli are modified rather than being occluded, the resultant effects are different. For example, when prism glasses were put on owls to shift their visual field 19º to the right, neurons in the inferior colliculus elaborated their dendrites into the adapted topographic space and clustered synaptic contacts there to accommodate the visual shift[99]. Such studies that manipulate sensory stimuli offer critical insight on how information encoded in different neural transmission influences brain circuit structural formation, and highlights the important role of competition for connectivity in directing axonal and dendritic growth.

In the central nervous system (CNS), sensory information is encoded into patterns of neuronal action potential firing and synaptic transmission between neurons. The main post-synaptic receptors that are involved in excitatory synaptic transmission are NMDARs and AMPARs, which are activated by the neurotransmitter glutamate. Modifying the function of these receptors alters the growth behavior of the dendritic arbor[100,101]. For example, NMDAR and AMPAR blockade in acute neonatal mouse cortical slices reduced the turnover and density of dendritic shaft filopodia[102]. Glutamatergic receptor blockade in RGCs of chick embryo retinal explants reduced filopodia length[103]. In *Xenopus laevis* tectum, blockade of NMDAR and AMPAR transmission resulted in destabilization and retraction of growing dendritic processes[30,104,105]. Moreover, NMDAR and AMPAR blockade in *Xenopus laevis* blocked the increase in growth of immature tectal neurons in response to visual stimulation[106]. Interestingly, excitatory glutamatergic synaptic transmission is required for dendritic arbor growth that is induced by sources other than synaptic transmission. For example, in the ferret visual cortex, BDNF-induced layer 4 pyramidal neuron dendritic arbor elaboration is dependent on both NMDARs and AMPARs[107].

Neuronal action potential firing also influences dendritogenesis. Increased extracellular potassium, which increases neuronal firing rate, increases dendritic growth in cultured rat cortical neurons[108].

Application of tetrodotoxin (TTX), a toxin that blocks voltage-gated sodium channels and prevents action potential firing and propagation, has variable effects on dendritic growth behaviors. For example, intracranial mini-pump infusion of TTX did not affect the arborization of neurons in embryonic cat lateral geniculate nucleus (LGN)[109]. Similarly, TTX did not affect dendritic arborization of young tadpole tectal neurons *in vivo*[104]. Chronic application of TTX in hippocampal co-cultures with glia did not affect afferent-induced dendritic arbor branching seen in controls[110]. However, TTX application to ferret cortical slices blocked neurotrophin-induced increased dendrite growth in pyramidal neurons, but not of neurotrophin-induced growth in inhibitory interneurons[107]. While TTX experiments have been used to understand the role of neural transmission in dendritogenesis, it is critical to recognize that while TTX blocks action potentials, it does not block all synaptic transmission because spontaneous vesicular release remains. Furthermore, interpretation of experiments employing increased extracellular potassium or TTX application need to take into account that these manipulations affect all of the neurons within the system, and therefore eliminate the endogenous complexity of activity patterns of endogenous systems. Critically, such global manipulations eliminate competition between neurons and neuronal inputs.

More sophisticated genetic methods to control neural activity now allow restricted control at the level of individual neurons within circuits. Two such methods are <u>D</u>esigner <u>R</u>eceptors <u>E</u>xclusively <u>A</u>ctivated by <u>D</u>esigner <u>D</u>rugs (DREADD) and optogenetics. In the DREADD approach genetically engineered G-protein coupled M3-muscarinic receptors have been modified to bring about either depolarization or hyperpolarization of an expressing neuron in the presence of CNO, a biologically inert drug[111]. In the optogenetic approach, receptors are activated by a particular wavelength of light and depending on the receptor can depolarize or hyperpolarize neurons (for discussion see

[112,113]). Both of these tools allow for more precise targeting of either neuronal populations or individual neurons since they are genetically based. Furthermore, optogenetics allow very precise control over neuronal firing rate, including patterns of depolarization. However, these tools have not yet been applied to the study of dendritogenesis and will not be discussed further.

1.7 Competition

It is now well established that activity plays a critical role in directing dendritogenesis and in establishing patterns of connectivity of developing neural networks. However, the concept of 'activity' is more complex than simply increased or decreased neural firing or transmission. Rather the pattern of activity and the information content it carries is important. Furthermore, it is critical to understand that activity influences development through its role in mediating competition between synaptic connections[30,114,115]. As a neuron searches the environment for synaptic partners, other neighboring neurons compete for the same synaptic partners. Synapse formation is necessary for the survival of growing neurons, since trophic factors from synaptic partners are required to prevent apoptotic cell death. The concept of a role of competition in directing neural circuit structural development was originally presented by Hubel and Wiesel from their observations that ocular dominance columns in cat visual cortex form unequally when kittens experience monocular deprivation but form normally when they experience binocular deprivation[92–94]. Subsequent work by the Stryker lab revealed a cellular contribution to Hubel and Wiesel's seminal findings by demonstrating that monocular deprivation alters the extent of arborisation of axons from the dLGN thalamic nuclei terminating in layer 4 of primary visual cortex. Axonal terminal arbors from the sutured eye were diminished, and those from the open eye had expanded territories[116,117]. More recent experiments using genetic expression of proteins that alter neural transmission in zebrafish support the model that competition between axons based on levels of activity influences growth.

When either an exogenous potassium receptor that prevents action potential firing or a dominant-negative SNARE protein, which blocks neural transmission was mosaically expressed in subsets of RGC axons in zebrafish, both net growth and the formation of new branches was strongly inhibited[114]. When the activity of nearby competing RGC axons was also suppressed, this inhibition was relieved. A similar effect of competition has been observed in the growth of dendritic arbors of *Xenopus laevis* tectal neurons[30]. Global administration of APMAR blockers in early development did not influence dendritic expansion[104]. Conversely, reducing synaptic AMPAR expression, producing weakened synapses in a single growing neuron in the optic tectum resulted in a less complex dendritic arbor[30]. The difference between these two experimental conditions was whether the AMPAR blockade was global or at the level of a single cell. Moreover, when plasticity-inducing visual stimuli were given, which promotes dendritic arbor growth of control tectal neurons, individual neurons with weakened AMAPR transmission actually retracted[30]. This demonstrates that during periods of heightened neural activity driven by sensory experience, states of competition are enhanced and the cells that are able to undergo LTP or form synapses win in the competition for presynaptic partners and grow, while neurons with weak synapses lose competitions and retract dendrites. Such experiments employing single-neuron manipulations elegantly demonstrate the importance of competition in activity-dependent growth. In contrast, this critical competition is lost in experiments using global blockade of activity that eliminates any difference in activity patterns between neurons.

1.8 *Xenopus laevis* as a model organism of early brain development

Xenopus laevis, also known as the African clawed frog, has become a classic model organism for studies of early development, both for ontogeny and the early steps in the development of the central nervous system due to its ability to generate and fertilize eggs year-round. The transparency

of naturally-arising albino mutant strains has allowed for direct *in vivo* imaging of the developing brain in *Xenopus*, and have led for it to become a leading model system for investigations of early brain circuit formation. In the 1960s Roger Sperry conducted seminal studies in *Xenopus laevis* on pathfinding of RGC axons from retina to tectum, providing critical evidence for the chemoaffinity model of axonal guidance[118,119]. In the late 1990s, Moo-Ming Poo employed the *Xenopus laevis* retinotectal circuit to provide important evidence for the spike-timing-dependent plasticity (STDP) model of LTP[120]. These studies and others have shown that the developing *Xenopus* brain system shares cellular and molecular mechanisms underlying neuronal maturation and circuit formation with mammalian systems supporting *Xenopus* tadpoles as a useful model for studying general properties of early brain circuit development.

Most of the studies of early circuit development in *Xenopus* examine the retinotectal system, in which RGC axons project to the contralateral optic tectum, corresponding to the superior colliculus in mammals, which is the primary visual area in frog and fish brains capable of processing visual stimuli[121]. As described by Sperry's Chemoaffinity Hypothesis[118], patterning of RGC projections to tectum establish a rudimentary retinotopic map guided by gradients of guidance cues in tectum and gradients of receptor expression in RGCs. Over time, as the tadpole matures the RGC axonal terminal arborizations refine to encompass a reduced proportion of the tectum[122]. Postsynaptically, this change is reflected as a decrease in the receptive field size[123]. It is believed that pre- and postsynaptic refinement driven by activity-dependent competition directs this circuit maturation[124].

Characteristics that make the retinotectal circuit of *Xenopus laevis* tadpoles a powerful model for investigating brain circuit formation include a protracted maturation spanning ~2 weeks, in which new neurons are added at proliferative zones in both the retina and tectum. The medial tectal

proliferative zone creates an age-ordered gradient of cell body layers allowing targeting cells at specific maturational states, which then grow into a functional, although developing, visual circuit. Furthermore, the accessible dorsal position of the tectum directly under the skin make the tadpole optic tectum particularly useful for *in vivo* studies of neuronal morphological and functional development and integration into circuits. Use of transparent albino *Xenopus laevis* tadpoles allows direct imaging access to this unperturbed, intact developing brain. Another important feature of this organism is the ease of immobilization during imaging experiments without anaesthesia, which would inherently interfere with normal neuronal transmission and endogenous activity-dependent plasticity mechanisms[125].

Two recently developed techniques, single-cell electroporation and two-photon microscopy, have contributed to making this system a leading model for the study of early brain development. Single-cell electroporation is a technique that is used to deliver macromolecules, including DNA, to individual cells within intact tissue[126]. This technique is particularly useful for differentiating between cell-autonomous versus global treatments or effects of experimental manipulations[30]. Two-photon microscopy allows *in vivo* imaging up to a millimeter into tissue with reduced photo-toxicity compared to confocal microscopy[127,128], and for time-lapse imaging at timescales ranging from seconds to days[10,29,106]. By combining these two techniques, it is possible to label a single neuron with a space-filling fluorophore and observe its morphological changes as it grows and integrates into functional circuits. Furthermore, high-resolution three dimensional images captured by two-photon microscopy allow accurate morphometric measurements of neuronal structures. Acquiring series of time-lapsed images can be used to observe dynamic changes of these structures during growth. Given the well-defined proliferative zone in the optic tectum, it is possible to

characterize neuronal growth throughout its development and identify the molecular mechanisms underlying developmental plasticity.

1.9 Research aims and hypotheses

The role that sensory activity plays in neuronal development has been a topic of great interest. However, while studies have established that sensory activity is critical to neuronal development, the precise effects have not been clearly elucidated. Furthermore, many studies have looked at the effects of activity modification after many hours or days, rather than looking at the more rapid growth behaviors that culminate in longer-term growth patterning. For this work I have contributed to the development of technologies for capturing such rapid dendritic arbor growth behavior in the awake developing brain and have applied them to more fully understand the relationship between dendritic arbor growth and functional plasticity of brain neurons.

Aim 1: To develop and optimize methods for transfecting single neurons in vivo based on the neurons functional characteristics.

Aim 2: To determine the relationship between dendritic arbor growth and functional plasticity during refinement.

Aim 3: To characterize activity-dependent and –independent dendritogenesis.

Chapter 2: Optimizing Targeted Single-Cell Electroporation

2.1 Introduction

Single-cell electroporation (SCE) is a powerful technique for delivering charged macromolecules into individual cells within intact tissues[126]. SCE is highly versatile due to both the range of compounds that can be delivered into cells and lack of limitation to the type of cell that can be targeted. This method restricts electroporation to a single cell by using a pulled glass pipette electrode to restrict both exposure to the poration-inducing electric field and the delivery compound in the pipette solution to the cell adjacent to the pipette's tip. Therefore, the only limitation for targeting neurons for electroporation is accessibility to the glass electrode. SCE can be used to fluorescently label neurons in vivo by the delivery of fluorescent dyes or by the delivery of plasmid DNA encoding protein fluorophores. Since combinations of compounds or different plasmids can be co-delivered, neurons can be labeled for fluorescent imaging while also expressing other markers, such as synaptic labels, or while manipulating molecular pathways.

Selection and targeting of neurons for SCE is an important aspect of this technique. In the simplest application, the SCE pipette is inserted into a region of tissue known to have a high concentration of the target neuron cell bodies, providing rudimentary neuronal type selection. However, targeting a region does not guarantee that a specific neuronal type will be electroporated, it only increases the likelihood. This approach, called 'blind SCE' typically involves use of low magnification microscopy which prevents direct visualization of target cells or pipette-tip interactions. Blind SCE can be useful if the location of target cells is known and their concentration is high.

Improved efficiency and targeting can be achieved using high-magnification infra-red (IR) microscopy to visualize the pipette tip-cell interactions. This 'targeted SCE' with IR video microscopy has been used for SCE of neurons in slices[129]. Visual-guided SCE opened the door to very precise electroporations of neurons that were hand-picked by the researcher. Furthermore, since the neurons could be visualized concurrently with electroporation, the morphological characteristics of the neuronal somata, and to a limited extent the shape of the dendritic arbor, could be used to identify the neuronal type before electroporating the cell, refining the targeting ability while using SCE. However, this type of refined targeting was limited to *in vitro* preparations as light scattering by tissue made the use of this approach inefficient *in vivo*.

Two-photon microscopy has been an important advance to combat this light scattering challenge. When the pipette tip is filled with a florescent dye, two-photon microscopy can be used to visualize the glass microelectrode. Furthermore, applying small quantities of positive pressure through the pipette injects small amounts of the dye solution into the extracellular space within the surrounding tissue, allowing the researcher to visualize the somata in the region which appear as dye-excluded shadows[130]. Using two-photon visual guidance, one can relatively easily position the SCE pipette tip against a target cell for high-efficiency loading of delivery compound. As a result, the extent of targeting previously achieved in culture could now be achieved *in vivo*. However, the selection criteria is still limited with this technique, based on cell soma shape. Alternatively, a researcher could use transgenic animals in which the neurons of interest express a cell-type specific genetically-encoded florescent protein.

While these methods for targeted SCE allow powerful selection criteria of specific neuronal targets, they do not allow selection of neurons based on functional properties. Recent *in vivo* functional imaging experiments now make clear that even neurons within the same sub-type, or

class, can respond to distinct sensory stimuli and therefore differ in their contribution to circuit function[131]. The importance of this complexity has become evident in interpretations of experiments examining activity-driven brain circuit development. These experiments traditionally employ altered sensory stimuli to test impact on brain neuronal growth[30,106]. However, no attempt is taken to relate sensory stimuli to the specific tuning of neurons examined. To address this problem, I have developed a novel SCE targeting strategy based on the functional characteristics of neurons *in vivo*.

In this chapter I will present a novel method for targeted SCE based on neuronal encoding properties. Measures are described that allow accurate prediction of the success of this SCE technique for transfection of plasmid DNA. This chapter is presented in a format appropriate for publication in the journal Nature Protocols, where this work will be submitted.

2.2 Experimental design

2.2.1 Choice of brain region

Imaging was done in the optic tectum, about 100µm under the surface of the skin. This is the region of the tectum that is rich in on/off responsive neurons. This technique can be used with any region accessible to two-photon imaging and a glass pipette.

2.2.2 Recording chamber

We use custom designed chambers that immobilize the head of the tadpole while leaving the tail in a chamber that is constantly perfused with oxygenated 10% Steinberg's solution (Fig. 2.1).

2.2.3 Choice of plasmids

Plasmid choice is open, this technique can be used to electroporate single plasmids or combinations of plasmids.

2.2.4 Electroporation parameters

For isolated pyramidal neurons in *Xenopus laevis* tadpoles, 60 square -30V pulses of 400µs duration at a frequency of 200Hz are effective parameters for DNA and 12 square +18V pulses of 200µs at a frequency of 900Hz are effective for Alexa flour 594. The electroporation parameters should be optimized for each cell type and experimental condition by varying the amplitude and number of pulses. Success rate in my hands is 55% for DNA and 90% for dye. Success rate was measured as the fraction of electroporated cells that were predicted and expressed the gene of interest 24 hours after electroporation. For dye, success rate was measured as the fraction of electroporated cells that had strong dye signal throughout their dendritic arbor.

2.2.5 Approach of cells under visual control

Cells can be targeted in two ways. If the cells are labelled with a florescent marker prior to approach, for example in transgenic animals or with previous whole brain electroporation, the florescent marker can be used to visualize the target cell. Alternatively, dye, or another fluorescent indicator, can be injected into the target brain region. This will allow targeting of cells by visualizing them by their 'shadow' in the injected dye.
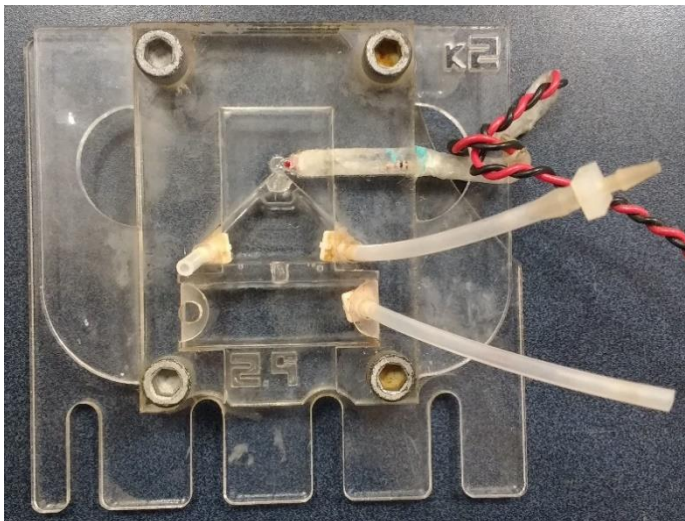
Figure 2.1: Recording chamber for imaging of *Xenopus laevis* tadpoles.

2.3 Materials

2.3.1 Reagents

- Experimental animals (here: *Xenopus laevis* tadpoles)
  ! CAUTION All animal experiments must comply with the relevant institutional and national care guidelines.
- Fluoroscent dye (Alexa Fluor 594 hydrazide)
- Oregon Green 488 Bapta-1 AM
- Plasmid DNA at a concentration of ~5μg μL^{-1}
- Anaesthetic (MS-222)
- NaCl
- KCl
- Ca(NO$_3$)$_2$
- MgSO$_4^-$ (7 H$_2$O)
- HEPES

2.3.2 Equipment

- Fine micromanipulator (e.g., Sutter Instruments Company ROE-200)
- Electroporation device (e.g., Axoporator 800A, Molecular Devices)
- Pipette puller (e.g., Sutter Instruments P97)
- Two-Photon microscope for in vivo imaging
- Water-immersion, high-numerical-aperture (NA) objective
- Fine brush
- Borosilicate glass capillaries
- Emission filters
- Tunable Ti:Sapphire laser
- Image acquisition software (e.g., LabView)
- Insect pin
- Fine tipped forceps
- Silver wire
- Transfer pipettes
- Stereomicroscope with long-working-distance air objective

2.3.3 Reagent setup

Steinberg's solution (1x)   5.8mM NaCl, 67μM KCl, 33.8μM Ca(NO$_3$)$_2$·4H$_2$O, 85.2μM MgSO$_4$·7H$_2$O, 1mM HEPES
Ca^{2+}-free Ringer's solution 11.6mM NaCl, 2.9mM KCl, 5mM HEPES
Oregon Green 488 Bapta-1 AM Dissolve 50mg Oregon Green 488 Bapta-1 AM in 4μL Pluronic F-127 in 20% DMSO to produce the stock solution. Dilute 0.4μL of the stock in 4μL Ca^{2+}-free Ringer's solution for working concentration.

2.4 Procedure

Preparation for dye injection into the tectum ● TIMING 5-10 minutes
1| Prepare dye to be injected into the tectum. For simple targeted single cell electroporation (TSCE) use any non-membrane permeable dye. For functional selection of cells use a

calcium indicator such as Oregon Green 488 Bapta-1 AM. I use 2.5mM Cascade blue for simple TSCE and 100mM OGB-1AM for functionally selected TSCE.

! CAUTION The dye should be diluted using calcium-free Ringer's solution.

2| Pull a thin and long-tipped borosilicate glass micropipette and fill it with 3-5µL of the dye solution.

3| Using a stereomicroscope with a long working distance air objective visualize the tip of the pipette. Use fine tipped forceps to break back the tip of the pipette creating a small opening. Apply 2-5 bar pressure to confirm that the solution flows.

▲CRITICAL STEP If the tip is not thin enough or is broken back too much, the rate of fluid flow through it will be too high and the tectum will be damaged. The solution beading at the tip is a good indication of correct flow rate.

Dye injection into the tectum ● TIMING 2 minutes per tadpole

4| Anaesthetize the tadpole by placing it into a 0.02% MS-222 solution for ~1 minute.

►SUGESTION start anaesthetizing the next tadpole while injecting this one, by the time you are done with the first tadpole, the second tadpole will be anaesthetized.

5| Place the tadpole on a wet paper towel on the microscope stage dorsal side up. If the tadpole is upside down, a paintbrush can be used to carefully flip the tadpole.

6| Use an insect pin to puncture the skin laterally of the optic tectum.

▲CRITICAL STEP It is very important to advance the insect pin very carefully. Failure to do this may result in the insect pin penetrating the heart. If any bleeding occurs, move on to the next tadpole.

7| Guide the tip through the punctured skin and up to the tectum. Slowly advance the tip against the tectum, you will see the dura dimple under the tip. Continue advancing the tip until the dura breaks. Gently tapping on the back of the manipulator may help penetrate the dura. Once the dura is penetrated, rapidly withdraw the tip to be just inside the tectum. Penetrating the brain will cause fluid to leak into the ventricle compromising the injection.

8| Using a pressure of 2-5 bar inject the dye into the brain. There will be a darkness that spreads from the tip, the goal is to have this darkness fill the tectum.

▲CRITICAL STEP There will be some swelling of the tectum. If the walls of the tectum start to shift, stop injecting immediately. Injecting further may result in damage to the tectum. If the darkness has not spread to at least 70% of the tectum, move on to the next tadpole.

9| Withdraw the tip from the tectum and transfer the tadpole into a recovery dish.

■ PAUSE POINT Wait at least 15 minutes for the tadpole to recover. The tadpole should be fully recovered from anaesthesia before further manipulation.

10| Fill the electroporation pipette with 3-5µL of pipette solution that contains your plasmid DNA (0.5-0.7µg µL^{-1}) and fluorescent dye (200µM). This step should be done concurrently with any of the previous steps.

Puncturing the dorso-medio-posterior side of the ventricle ● TIMING 6 minutes / tadpole

11| Anaesthetize the tadpole by placing it in 0.02% MS-222 for 5 minutes.

►SUGGESTION Start anaesthetizing tadpoles ahead of time (if possible) as this will greatly reduce the time this step takes.

12| Transfer the tadpole into the imaging chamber, filled with 0.02% MS-222, and secure with coverslip and clamp.

13| Under the stereomicroscope use a sharp insect pin to puncture the dorso-medio-posterior side of the ventricle through the skin and the dura.

▲CRITICAL STEP Bleeding at the site of puncture in the skin makes is highly unlikely that the subsequent electroporation will be successful. Also, penetrating too deep through the dura will result in damage to the cells in the tectum.

? TROUBLESHOOTING

Targeted single-cell electroporation ● TIMING 3 minutes / tadpole

! CAUTION If this procedure takes more than 10 minutes, abort the experiment to avoid the tadpole waking up with a pipette tip inside the tectum. In case the procedure is taking too long consistently, consider perfusing with 0.02% MS-222 instead of aborting the experiment.

14| Transfer the chamber to the stage of the two-photon microscope and attach the perfusion system, ground electrode, and LEDs/screen (used when selecting neurons based on functional properties).

15| Using a low power high numerical aperture (10-20x, 0.8NA) water-immersion objective guide the tip through the hole at the back of the ventricle and up to the tectum. Switch to a high power high numerical aperture (40-60x, 0.8NA) water-immersion objective and find the tip.

? TROUBLESHOOTING

16| Switch to two-photon imaging. Locate the cell to be electroporated, move the tip outside the tectum so that it can be advanced directly at the cell with minimal lateral movement (no more than 10-20µm). Place tip at the center of the target cell ensuring that the tip and the cell are in the same focal plane.

? TROUBLESHOOTING

17| Electroporate the cell. The parameters will vary depending on the substance being electroporated and the cell type. For sample parameters refer to 'Experimental design – Electroporation parameters'.

▲CRITICAL STEP The quality of the electroporation can be qualitatively assessed during the electroporation (Fig. 2.3).

? TROUBLESHOOTING

18| The same pipette can be used to electroporate multiple cells. Restart at Step 16.

19| Transfer the tadpole to a recovery dish.

■ PAUSE POINT If dye was electroporated, wait for 20-30 minutes before imaging the electroporated cell. The dye persists for days within the cell (longest tested time = 4 days). If DNA was electroporated, wait for 1 or more days, depending on the type of DNA electroporated, for sufficient expression levels.

20| Assess expression of gene of interest.

● TIMING

Steps 1-3: Preparation for tectal pressure injection: 5-10 min
Steps 4-9: Tectal pressure injection: ~3 min per tadpole
Steps 11-19: two-photon targeted single cell electroporation: 5-15 min per tadpole

? TROUBLESHOOTING

Troubleshooting advice can be found in **Table 1**.
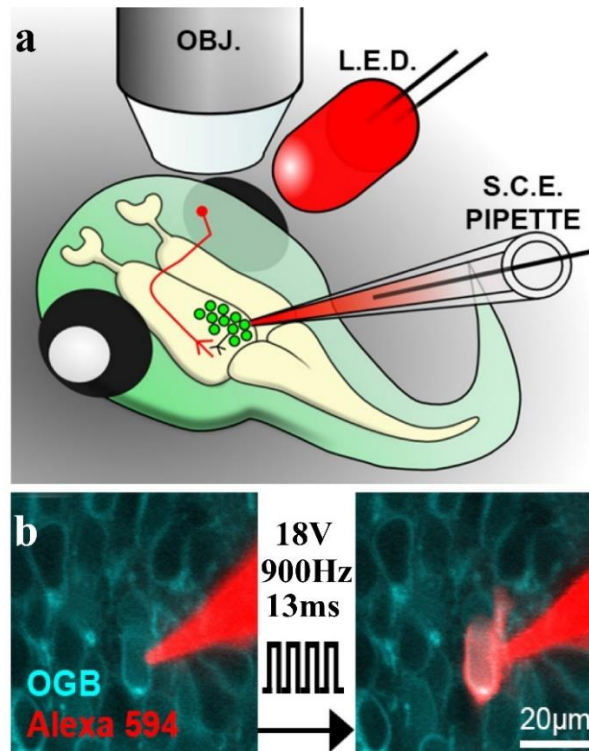
Figure 2.2: Targeted single cell electroporation.
a) A cartoon of the setup for targeted single cell electroporation of neurons based on their responsiveness to a sensory stimulus. The tadpole is visually stimulated to assess neurons for responsiveness. A selected neuron is then electroporated. **b)** Neuronal responses monitored by observing changes in intensity of Oregon Green Bapta 1 - AM (cyan). Panels from left to right show states before and after electroporation of a neuron with Alexa 594 dextran dye (red).
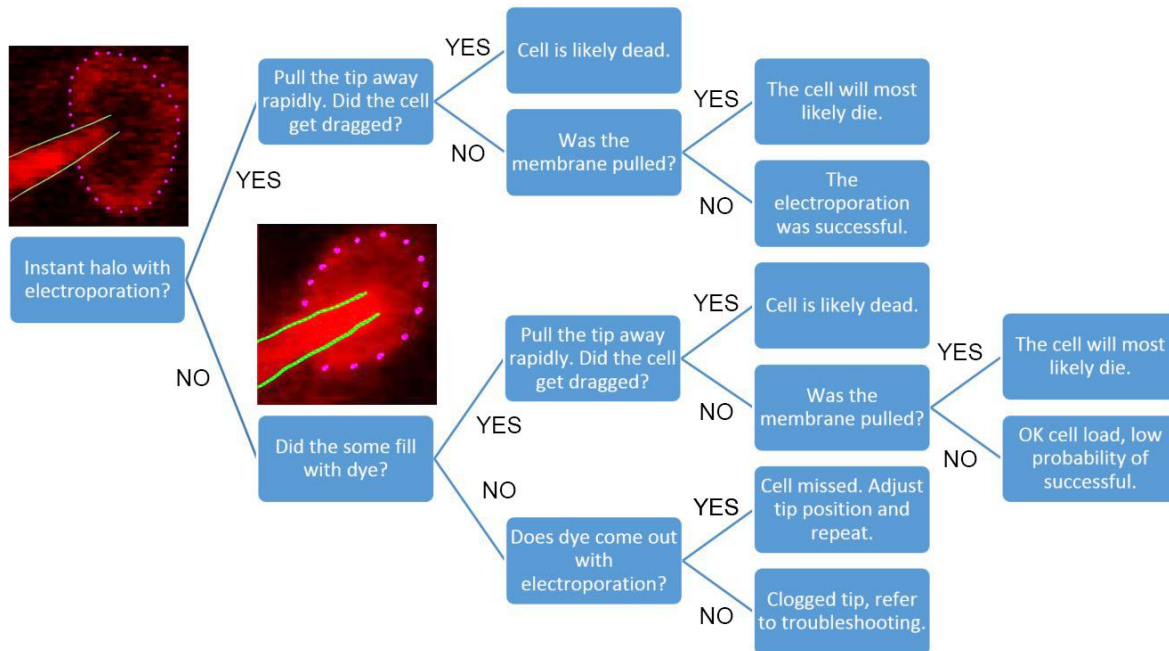
Figure 2.3: Flowchart for assessing the success of an electroporation.

2.5 Anticipated results and conclusion

Using Oregon Green 488 Bapta-1 AM made the selection of neurons based on their tuning possible. However, the densely packed neuronal somata in the *Xenopus laevis* tadpole optic tectum pose a challenge to electroporation. An experienced experimenter can reliably electroporate plasmid DNA with a confidence of 55% that the gene-of-interest will be expressed if the electroporation was predicted to succeed. For Dye, the confidence that an electroporation will produce strong signal throughout the dendritic arbor is 90%. Thus, targeted single cell electroporation can be used to selectively label individual neurons of a particular identity, even in regions of multiple nearby somata *in vivo*.

Table 2.1: Troubleshooting advice

Step	Problem	Possible reason	Solution
13	Tadpole starts bleeding when hole is poked	Nicked vein	This tadpole can still be used, however the probability of tip clogging increases
15	Cannot locate the hole with the 10x objective	Poor hole; Lack of experience	Practice will resolve this issue. In the meantime, move on to the next tadpole. Alternatively, 'rake' the skin in the vicinity of where the hole should be with the pipette tip. NOTE: 'raking' will increase the chances of clogging the tip
15	Once switched from the 10x to the 60x objective, the tip is always 'just' out of focus	The objective is touching the pipette	The objective is hitting the pipette tip as a result of the angle of the arm holding the pipette tip being changed. Adjust the angle of the arm.
16	When tip is moved inside the tectum, the tectum moves with the tip	The tip is bumping into or is caught on the skin	Either the hole is poor or it's positioning is poor. Move on to the next tadpole. If problem persists, practice making holes
16	There appears to be a void around the tip. When the tip is moved towards cells, the cells seem to disappear	The tip did not go through the dura.	This is either a result of not poking a hole through the dura, or missing the hole with the tip. Attempt to put the tip in to tectum again (using the 10x objective). If this does not resolve the issue, move on to the next tadpole.
16	When moving the tip in the tectum the tip does not move or moves only in large increments	The pipette is likely hitting the edge of the hole in the coverslip, the perfusion tubing or another part of the chamber.	Adjust the pieces of the chamber.
17	No dye coming out of the pipette tip	The tip is either clogged or insufficiently strong stimulation parameters are being used.	Check the parameters first. If problem persists, try unclogging the tip by stimulating with a very high voltage pulse (take the tip out of the tectum, into the ventricle for this). If problem still persists, change tips.
17	Clusters of neurons are electroporated	Electroporation parameters are too high; tip is positioned near two cells	Decrease either the potential or the train length, or both. Alternatively, ensure that the tip is positioned in the center of the target neuron.
17	Neurons are electroporated but are too dim	Sub-optimal electroporation parameters	Increase either the potential or the train length, or both, until clusters are being electroporated, then go to the highest parameters that did not result in a cluster.

Chapter 3: Relationship Between Dendritic Morphology And Functional Plasticity

3.1 Introduction

As neurons mature they concurrently elaborate their dendritic and axonal arbors and functionally integrate into circuits. Sensory experience is thought to contribute to the selection of the circuits that will become more refined since it is these circuits that are most likely to be relevant to the animal. The effects of learning on the structure of neurons have begun to be characterized. For example, when rats are repeatedly taught a motor task, neurons in the motor cortex develop new spines on their dendritic arbors[132,133]. When the behavior becomes extinct, those spines disappear. Similarly, rearing owls with prism glasses results in neurons expanding their dendritic arbor into the correct retinotopic space to accommodate for the shift in visual field[99]. Furthermore, other studies suggest that functional plasticity of individual dendritic processes is correlated with structural plasticity. When activity in a hippocampal slice is blocked and then the blockade is locally lifted while inducing LTP in the spines of the same region, new spines appear only in the disinhibited region when LTP is induced in that region[134]. Similarly, when dendrites are stimulated with LTP inducing tetanic stimulation with an electrode, filopodia begin to grow in the region, with the increased growth rate persisting for up to 40 minutes[135]. Here, I investigated the relationship between structural plasticity of the complete dendritic tree of a neuron *in vivo* while inducing functional plasticity in that same neuron.

Functional properties were identified and tracked by acquiring somatic calcium indicator traces. Previous research has shown that calcium indicators can be used to monitor individual action potential firing and action potential burst firing. In fact, the amplitude of the calcium transient is

an indicator of how many action potentials were fired in a burst[131,136]. Using this property, by measuring the amplitudes of somatic calcium traces I was able to identify the plastic shift of the cells under investigation. Increases in amplitude were interpreted as potentiation of the firing output and decreases in amplitude as depression of the firing output.

To monitor the structural plasticity, the volume that a neuron occupies was imaged over time. Then, a custom-written software called 'Dynamo' was used to trace the neuron and provide an identity to each component part of the dendritic arbor so that changes to any given structure could be monitored. The process of measuring a neuron over time and monitoring changes is termed 'dynamic morphometrics'. Dynamic morphometrics is a powerful technique because all changes to the dendritic arbor can be monitored and precisely and easily tracked. This in turn provides a wealth of information about how the neuron's structure is changing over time.

In this chapter I will present the work that focused on identifying how patterns of functional plasticity correlate to the patterns of structural plasticity. This was achieved by teaching a tadpole to better discriminate a visual stimulus while concurrently measuring how visual tectum neurons' dendritic arbors change and the functional plasticity that those neurons undergo.

3.2 Methods

Animal rearing, calcium indicator loading and targeted single-cell electroporation were performed as described in Chapter 2.

3.2.1 Experimental protocol

Visual stimuli were presented via a 635nm LED (LTL-709E, Lite-On Inc.) placed against the eye contralateral to the imaged tectum. Visual stimuli consisted of OFF flashes. An OFF flash is defined as the LED initially being on and then being turned off for 50ms before being turned on

again. Probing consisted of OFF flashes presented once a minute. Spaced training (ST) consisted of three 5-minute bursts of high-frequency (0.25Hz, 50ms) OFF flashes spaced by 5 minute periods of invariant light and had been previously shown to affect neuronal plasticity[137].

The experimental protocol consisted of four stimulation segments and five morphology imaging segments. The morphology segments were before the first stimulation segment, between stimulation segments and after the last stimulation segment. The first, third and fourth stimulation segments were probing, while the second stimulation segment was ST.

3.2.2 Neuron selection

For all experiments, we targeted type 13b pyramidal neurons in the dorsolateral tectum of stage 50 tadpoles[67]. These neurons show robust visually evoked responses and are relatively stable morphologically, with motility rates that can be accurately captured by 30-minute imaging, at this stage in development.

3.2.3 Plasticity blockade

For experiments where D-APV (50µM) was applied, it was injected before imaging in Ca^{2+}-free Ringer's solution containing OGB, and then again in Ca^{2+}-free Ringer's solution between the first epoch and spaced training, prior to training onset.

3.2.4 Two-photon imaging

Two-photon imaging was conducted with a scan-mirror based two-photon microscope adapted from an Olympus FV300 confocal microscope and a Chameleon XR Ti:Sapphire laser (Coherent). Single cells and their neighbors were imaged at 6.6Hz in a 28x28µm field of view over 20s, 10s pre-stimulus and 10s post-stimulus.

3.2.5 Analysis

Custom software called "Dynamo" was used to analyze both the morphology and activity of neurons. For morphology, the dendritic arbor was manually traced using Dynamo. The analysis was then based on the drawn structure. This process allowed for precise measurement of all filopodia in the dendritic arbor, including changes in branch and filopodial length over time. For activity analysis, cell of interest, as well as surrounding cells, were manually identified from a projection of the 20s movie. A trace of pixel saturation within the area occupied by the neuronal somata is then used to identify the amplitude of the calcium transient. Amplitudes of calcium transients are used to quantify neuronal responsiveness and plasticity.
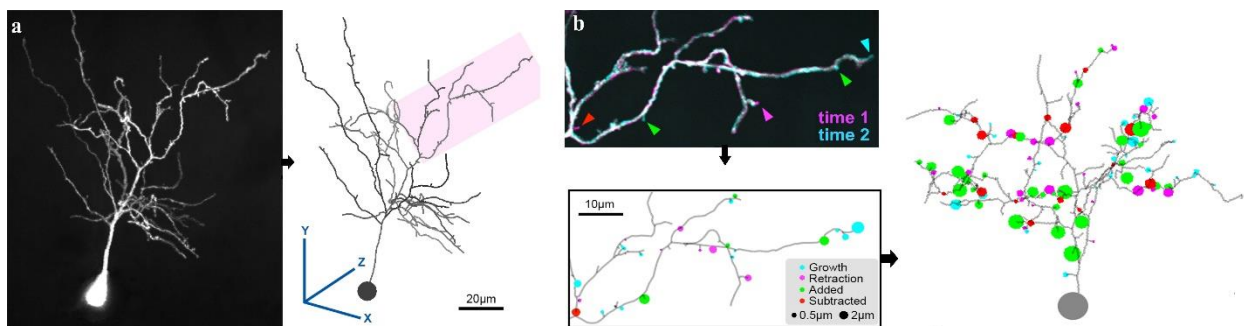
Figure 3.1: Reconstruction and morphometrics of a neuron with Dynamo.
a) Left panel shows a Z-projection of a neuron image stack while the right panel shows a 3D reconstruction in the Dynamo software. **b)** The top left panel shows an overlay of two image stacks acquired 30 minutes apart. The overlay is white where structures are stable, cyan where they extend, and magenta where they retract. Arrowheads mark sites of addition (green), subtraction (red), growth (cyan) and retraction (magenta). The bottom left panel shows a motility plot representing the same changes. The right panel shows what a full reconstructed neuron with all changes looks like.

3.3 Results

For this set of experiments neurons were selected based on their action potential tuning responses to an OFF stimulus. Tectal neurons were targeted for SCE if they demonstrated somatic action potential burst in response to an LED, near the contralateral eye, being turned off for 50ms. These were called '**Responsive**' neurons. SCE delivered a space-filling morphological indicator and imaged using in vivo two-photon time-lapse microscopy in awake tadpoles. As controls, a second

set of neurons were targeted for SCE if their somata were neighboring OFF responsive neurons, but they did not fire action potentials in response to OFF ('**Non-responsive**' neurons).

Neurons were grouped according to their initial somatic response to OFF stimuli during baseline recording and changes in calcium transient amplitude following ST: **LTP** – an initial response that increased with training (n = 7; Fig. 3.2), **No Change** – an initial response that did not change (n = 4; Fig. 3.4), **Become Responsive** – no initial response but a response after training (n = 3; Fig. 3.3), **No Response** – no response before or after training (n = 6; Fig. 3.4). Each group showed distinct experience-driven neuronal growth, with activity profiles explaining most of the variation in growth patterns (65%, MANOVA F, p<0.01). Growth patterns that were quantified include addition rate, subtraction rate, and motility of filopodia, as well as filopodial lifetimes and clustering of growth behaviors.
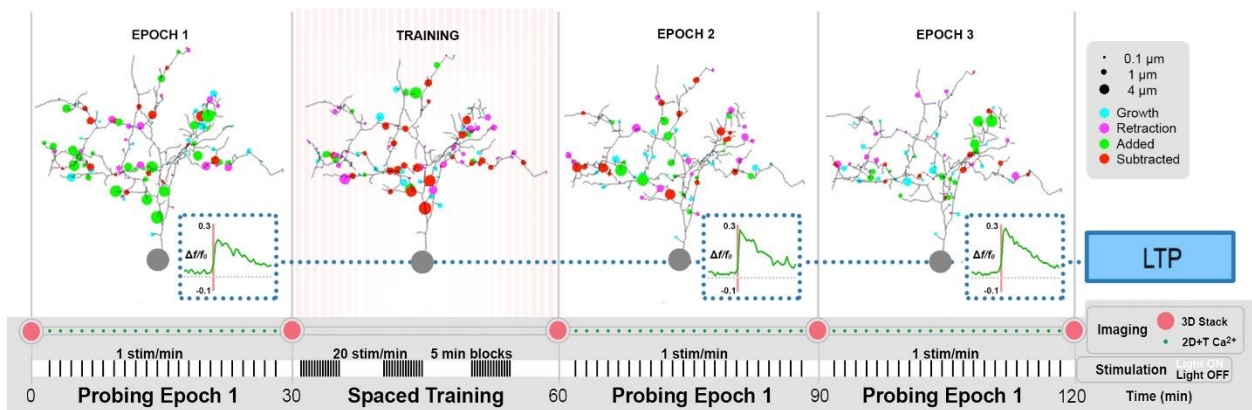
Figure 3.2: Neurons that potentiate tend to prune with training.
Dynamo motility plot of the LTP activity profile (LTP - initial response that gets larger after training). Inset shows mean evoked responses ($\Delta F/F_0$).

3.3.1 Experience-induced dendritic growth patterns are correlated with evoked somatic activity and plasticity

Neurons that potentiated, **LTP** neurons, showed an increased rate of subtraction of filopodia in response to training that gradually returned to baseline over an hour after training. The addition rate of filopodia for the **LTP** neurons decreased with training and remained low over the next hour

(Fig. 3.6). In **LTP** neurons, motility follows a similar trend, with less extension and more retraction overall (Fig. 3.7). Neurons belonging to the **No Change** group showed a persistent decrease in the addition rate following training and no significant changes in subtraction rate (Fig. 3.6) or motility (Fig. 3.7). **No Response** neurons showed an increase in the addition rate during training (Fig. 3.6). The motility mirrored the additions with a slight increase in extensions during training (Fig. 3.7). **Become Responsive** neurons showed an increased rate of additions during training that gradually returned to baseline levels over the next hour, and a strong and persistent increase in subtractions after training (Fig. 3.6). In addition, **Become Responsive** neurons showed an increase in the magnitude of filopodia extensions during training (Fig. 3.7). Across groups survivalship rates of filopodia are consistent with the exception of the filopodia of LTP neurons that are born during and within 30 minutes of training, more of which survive over an hour than in any other group (Fig. 3.8). Here I have shown that neurons belonging to each profile have a distinct growth pattern in response to training. Overall, potentiation of the somatic response is associated with filopodial pruning, while absence of a somatic response was associated with growth during training.
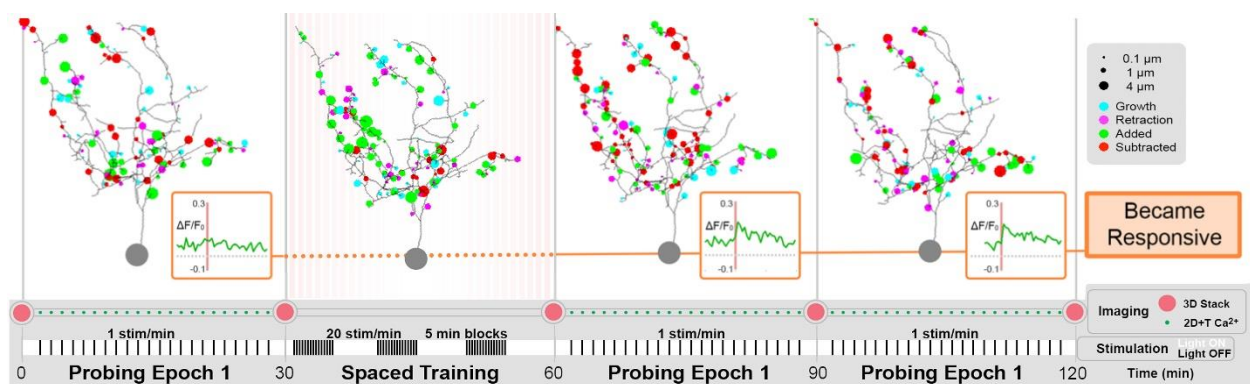
Figure 3.3: Neurons that gain a response with training first grow and then prune.
Dynamo motility plot of the Became Responsive activity profile (Became Responsive - no initial response but a response after training). Inset shows mean evoked responses ($\Delta F/F_0$).
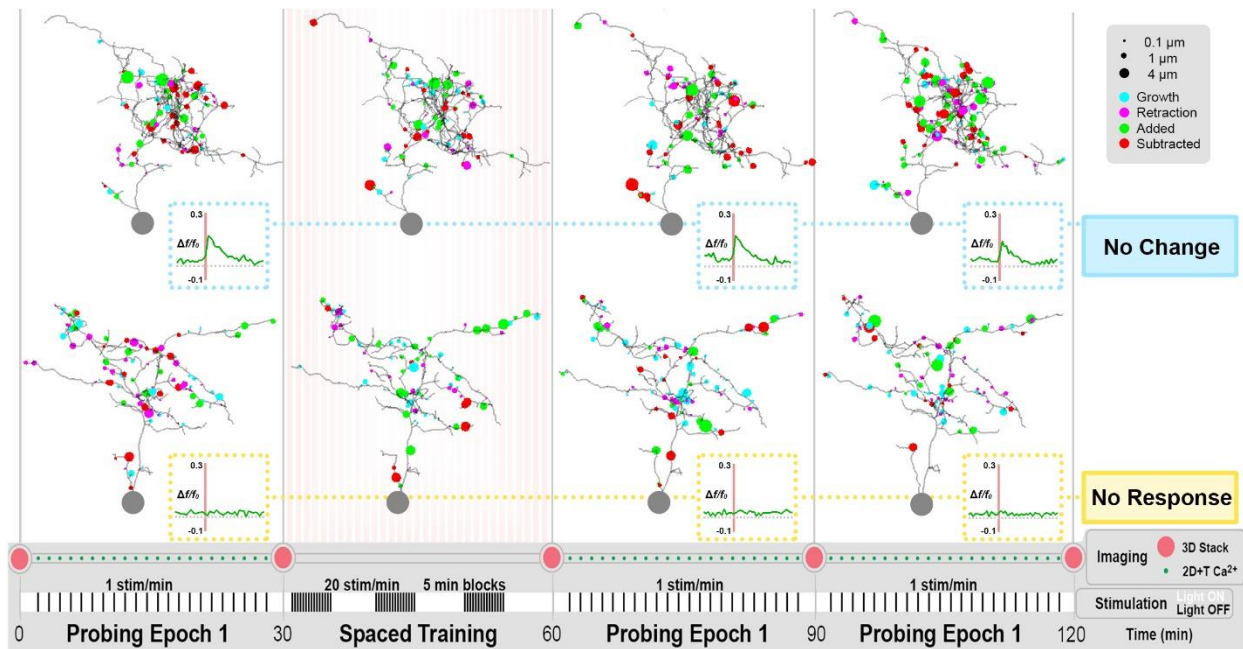
Figure 3.4: Dynamo motility plots and mean evoked responses of No Change and No Response activity profiles

No Change – initial response that remains unchanged with training. No Response – no response before or after training. Inset shows the mean evoked responses ($\Delta F/F_0$).
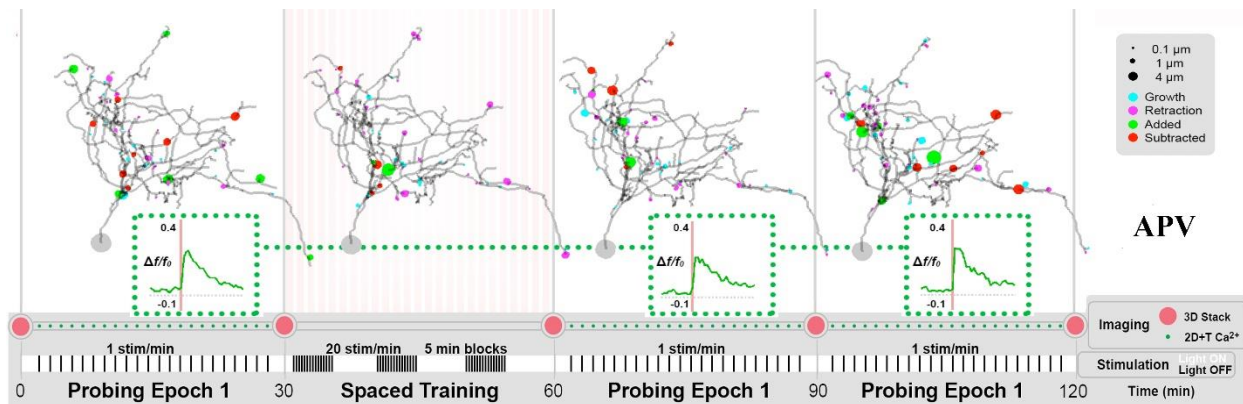
Figure 3.5: Dynamo motility plot and mean evoked responses of neurons perfused with NMDA receptor blockers.

Inset shows mean evoked responses ($\Delta F/F_0$).

3.3.2 Blockade of plasticity abolished differences in experience-induced dendritic growth patterns

In order to establish causality in the correlation between structural and functional plasticity established in the previous section, the experiments were repeated with the addition of D-APV (50μM). D-APV is a competitive NMDA receptor antagonist and has been shown to abolish functional plasticity when present during plasticity induction. When these experiments were

conducted in the presence of D-APV, training with ST visual stimuli did not have an effect on the

growth behavior of **Responsive** or **Non-responsive** neurons (Fig. 3.5, Fig. 3.6).
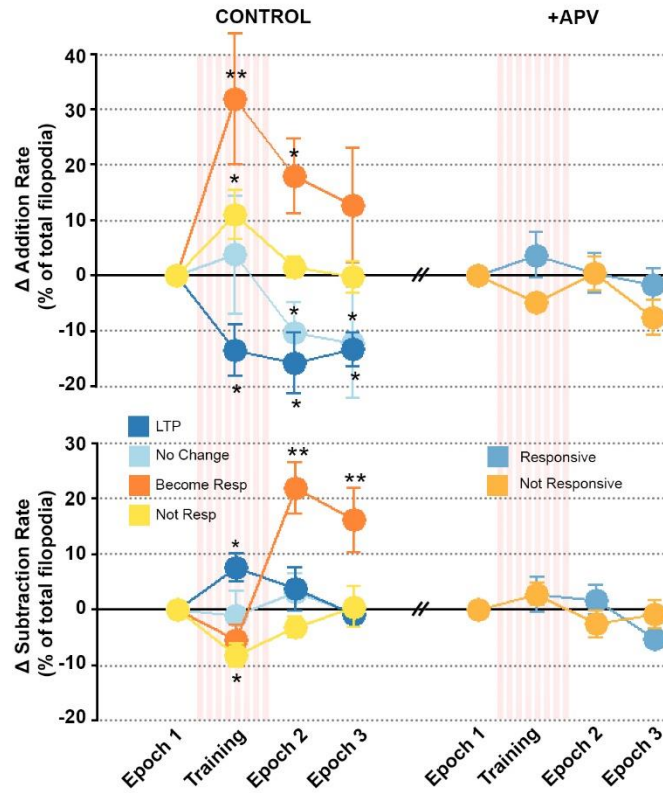
Figure 3.6: Mean addition and subtraction rates of filopodia.
From left to right, control neurons and neurons following D-APV injection. Rates are expressed as percent of total filopodia at Epoch 1, minus mean rate during Epoch 1. Control: N = 7 (LTP); 4 (NC); 5 (BR); 4 (NR). APV: N = 4 (R); 4 (NR). *p<0.05, **p<0.01, relative baseline of the same treatment. Errors bars are SE. Statistics are done with an ANOVA followed by Tukey LSD post-hoc test.
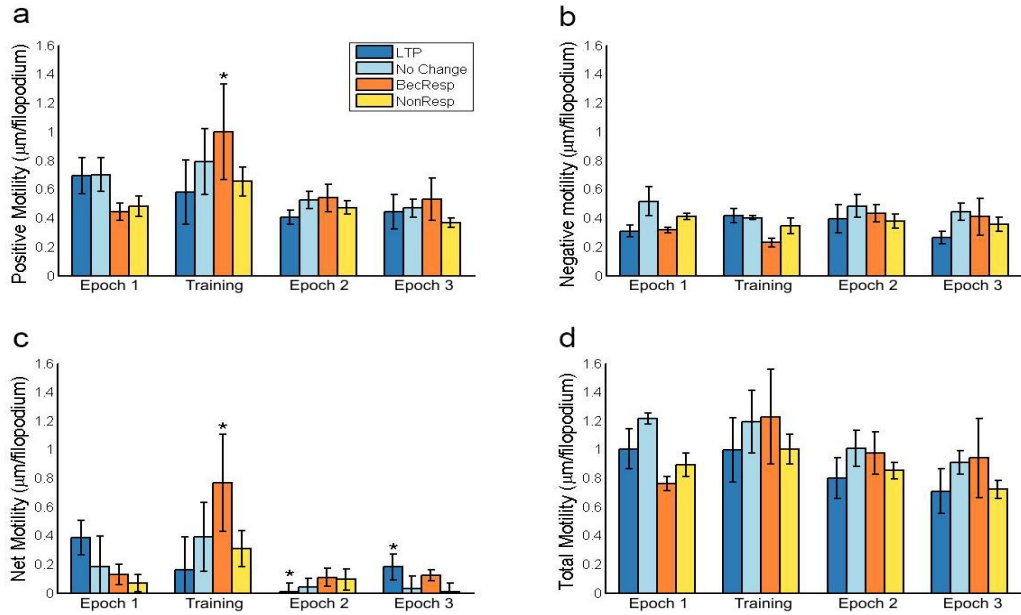
Figure 3.7: Mean rates for extensions and retractions of filopodia subdivided by activity profile.
Rates are expressed as mean changes in length of filopodia. **a**. Positive motility (extension of filopodium). **b**. Absolute value of negative motility (filopodium decreased in length but is still present). **c.** Net motility = positive motility + negative motility. **d.** Total motility = positive motility + absolute value of negative motility. N = 7 (LTP); 4 (NC); 5 (BR); 4 (NR). *p<0.05, compared to baseline (Epoch 1). Error bars are SE. Statistics are done with an ANOVA followed by Tukey LSD post-hoc test.
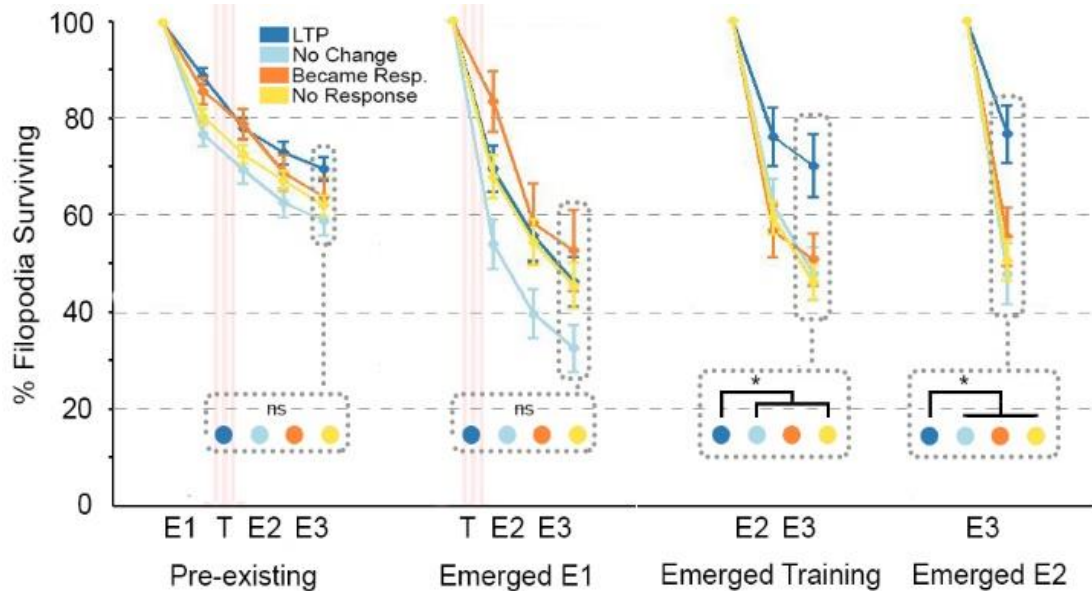
Figure 3.8: Filopodia survivalship over time, by activity profile.
Each filopodium was individually tracked to generate the survivalship over time curves. Data points represent the percent of filopodia that existed at the time specified at the bottom of the figure that survive to each of the times in the x-axis. N = 7 (LTP); 4 (NC); 5 (BR); 4 (NR). *p<0.05. Error bars are SE. Statistics are done with an ANOVA followed by Tukey LSD post-hoc test.

3.3.3 Neuronal positive growth behaviors are clustered

From the images of Dynamo motility plots it appeared that some growth behaviors were

clustered. By comparing the probability of distances between nearest filopodia sharing the same

growth behavior to expected distances generated by Monte Carlo sampling, clustering of

additions and extensions, but not subtractions or retractions, was revealed (Fig. 3.9). Both

additions and extensions were clustered within 5μm, while only extensions were clustered

between 5 and 10μm.
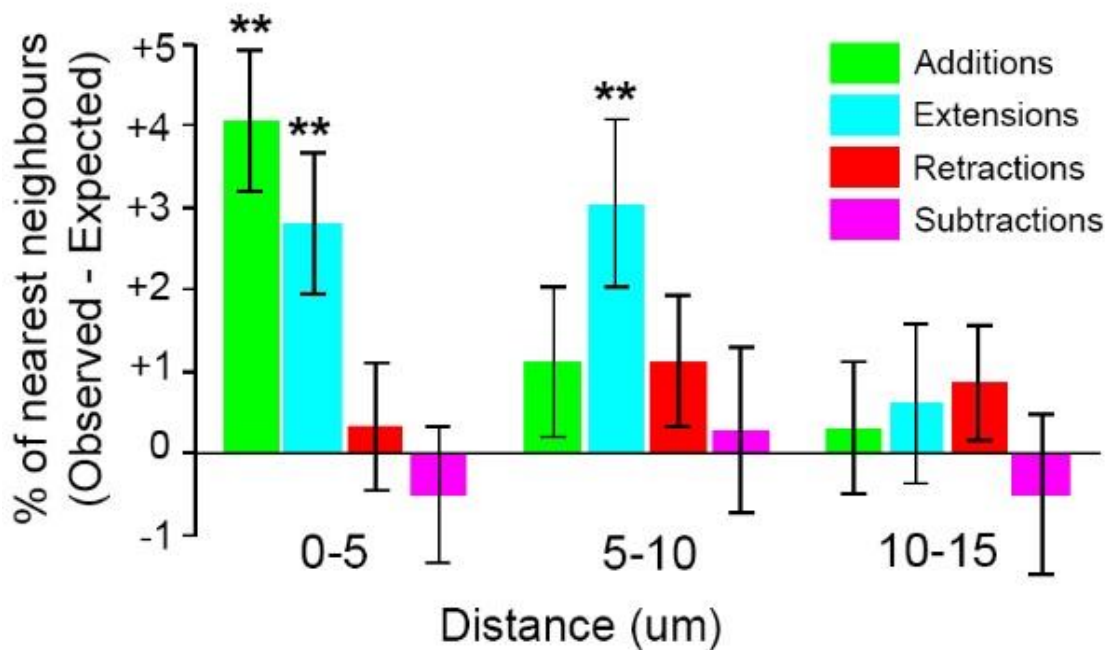
Figure 3.9: Filopodia additions and extensions are clustered.
For each filopodium of a given growth behavior the distance to the nearest filopodium of the same growth behavior was measured. Plotted are the observed probabilities of each distance minus the expected probabilities obtained by Monte Carlo sampling. Filopodial additions **(green)** and extensions **(cyan)** occur significantly closer together than expected by chance. Subtractions **(red)** and retractions **(magenta)** are not significantly clustered. N = 1504 additions, 1102 subtractions, 1264 extensions, 1175 retractions in 21 neurons. ** $p < 0.01$, Kolmogorov-Smirnov test.

3.4 Discussion

The functional and structural development of neuronal dendritic arbors reciprocally interact to

direct formation of the mature arbor. In this experiment individual neurons in the optic tectum of

albino *Xenopus laevis* tadpoles were co-labeled with a calcium-sensitive fluorescent dye and a space filling dye. The combination of dyes allowed the visualization of bursts of action potentials in the neuron, seen as calcium transients in the soma, and the entire neuronal dendritic arbor morphology. The neurons were then presented a visual stimulation protocol known to induce LTP of visual-evoked responses in the majority of tectal neurons. The correlation between activity-driven functional plasticity and neuron morphology was characterized.

3.4.1 Experience-driven dendritic refinement and maturation

When stimulated with high frequency OFF stimuli in a spaced training (ST) format, **Responsive** neurons decreased the addition rate of new filopodia below baseline levels. Separating the **Responsive** neurons into **LTP** and **No Change** plasticity outcomes, we observe that the decrease in additions is present in **LTP** neurons starting at the time of training and persisting for the next hour, while in **No Change** neurons the decrease is evident only after training. These results are in line with studies demonstrating that increased neural activity, which leads to synaptic maturation, inhibits dendritic outgrowth[44–46]. The decreased rate of additions of filopodia in **LTP** neurons suggests that ST drives maturation in these neurons since synaptic stabilization has been shown to be associated with morphological stabilization and decreased additions of filopodia[44–46]. Thus, decreased addition rate of filopodia in **LTP** neurons was seen as a consequence of the neuronal dendritic arbor becoming specialized to the OFF circuit to a point where new processes were not required for the functioning of the neuron within the OFF circuit. In the case of **No Change** neurons, the decrease in addition rate was observed only after training. Thus, while training does not appear to directly affect the addition rate, it appears to act indirectly. Since the onset of the decrease is on the order of half an hour following ST, it is possible that the mechanism by which training affects **No Change** neurons is transcription factor dependent. Possibly, the same

mechanism is responsible for the persistent decrease in addition rates in both **LTP** and **No Change** neurons.

Apart from a decreased filopodial addition rate, increased filopodial elimination was also observed in neurons that underwent LTP. Filopodial elimination is termed dendritic pruning. Dendritic pruning has been associated with potentiation of neurons, both *in vitro* and *in vivo*[138,139]. Here, pruning likely results from destabilization of synapses that are not stimulated by the LTP inducing OFF ST stimulus and serves to specialize the neuron to the OFF circuit by increasing the proportion of its synapses to this circuit. Since weak synapses tend to be dissolved, it is likely that **LTP** neurons specialize to the OFF circuit not only by strengthening existing OFF circuit synapses but also removing synapses connected to other, non-OFF circuits.

An interesting observation was that **No Change** neurons did not appear to prune either during or after training. These neurons are clearly integrated into the OFF circuit, as evident by their action potential responses to OFF stimuli. As such, these neurons likely already contain a large number of synapses that are part of the OFF circuit and few synapses that participate in other networks. With only a few inappropriate contacts pruning may not be required for these neurons to maintain their specialization in the OFF network. An alternative explanation is that because these neurons are so robustly integrated into the OFF circuit, driving the OFF circuit hyper-stabilizes these neurons, preventing additional modifications to their growth behavior. In either case, this observation is not unprecedented. When activity blockade was applied to a neuron and selectively lifted in order to induce LTP in the spines of the dendritic segment, changes in growth behavior were seen only when the stimulus induced plasticity[134].

Structural plasticity during neuronal development is characterized by an overshoot in synapse numbers[140] which are subsequently reduced to adult levels[141,142]. The results from this experiment

suggest that robust OFF stimulation evokes dendritic arbor refinement and maturation as described by the processes of dendritic pruning and synaptic strengthening. Given that the maturation was caused by the ST protocol, we concluded that LTP-inducing OFF stimuli accelerated the maturation process of the neurons that partially partake in the OFF circuit and transiently hyper-stabilized the neurons that are already specialized in the circuit.

3.4.2 OFF circuit activity drives seeking behavior in non-responsive neurons

When referring to **Non-responsive** neurons it is important to realize that at this stage of tadpole retinotectal circuit development all tectal neurons are relatively immature and form connections with many different circuits, functionally seen as having a large receptive field[131,143]. Therefore, the term **Non-responsive** does not preclude the presence of synapses with the OFF circuit. Thus, in this context, **Non-responsive** means that the OFF stimulation was not sufficient to generate action potentials in these neurons.

We observed that **Non-responsive** neurons showed a transient increase in addition rate of filopodia in response to ST. This finding agrees with the literature where LTP of a single spine induced the formation of more spines[134,144,145]. Generation of new spines was seen both when tetanic stimulation with an electrode was used to induce LTP, as well as activation of presynaptic neurons. Thus, the increase in filopodia additions is likely a consequence of the **No Response** neurons sensing the robust activity of the OFF circuit through synapses with that circuit and responding with seeking behavior in an attempt to form further connections with OFF circuit axons. This reasoning is supported by work that has shown learning to be associated with formation of new spines[132,133,146]. Furthermore, this type of behavior makes sense in terms of early brain development. It is during the early stages of development when animals often learn to process specific types of stimuli efficiently since these are the stimuli that are likely to be important

throughout their life. This line of reasoning is further supported by observing that the increased addition rate, seeking behavior, occurs only during training and rapidly returns to baseline after. Thus, only while a circuit is being driven robustly there is an active attempt to integrate into the circuit.

Further evidence for the idea that the increased addition rate is a reflection of seeking behavior exhibited by the neuron comes from **Become Responsive** neurons. These neurons show a similar pattern of growth behavior to **No Response** neurons with training, namely an increased addition rate of filopodia. However, in **Become Responsive** neurons training results in the acquisition of a response with training, after which point the subtraction rate increases greatly, a similar growth behavior to **LTP** neurons. Thus, it appears as though **Become Responsive** neurons behave as **No Response** neurons before they acquire a response and then start behaving as neurons that potentiated. This suggests that **Non-responsive** neurons seek to make contacts with the driven circuit and once sufficient contacts have been established begin to prune away contacts that are not relevant to the driven circuit. It is possible that the difference between **No Response** and **Become Responsive** neurons is in the initial number of contacts with the OFF circuit, or the relative density of OFF circuit axons in the vicinity of their dendritic arbors.

3.4.3 Functional plasticity is required for structural plasticity in response to training

In studies that have shown that functional and structural plasticity are correlated, blockade of NMDA receptors abolished the effects seen[106,134,135]. Similarly to the literature, when neurons underwent training in the presence of D-APV, an NMDA receptor antagonist that blocks plasticity if present during plasticity induction, in this experiment the effects of training were no longer seen. This was the case for both **Responsive** and **Non-responsive** neurons. This suggests that NMDA receptors are critical for experience-induced structural plasticity. In addition, since **No Response**

neurons did not show ST-induced modulation of growth behavior, and the non-responsive nature of these neurons suggests that only a few synapses integrated into the OFF circuit exist on these neurons, it appears that NMDA receptor activation at relatively few synapses is able to induce neuron-wide changes in structural refinement. Overall, the finding that NMDA receptor blockade abolished ST-induced structural plasticity suggests that functional plasticity is upstream of structural plasticity.

3.4.4 Protrusive growth behaviors are clustered

Multiple studies looking at the role of activity in neuronal development show that synaptic tuning has been observed in some neurons[133,147], raising questions of how this clustering arises. In this chapter the time-lapse imaging of a large set of neurons allowed me to monitor the growth dynamics of these neurons. I observed that additions and extensions of filopodia were clustered. It is possible that clustering of protrusive growth behaviors is the mechanism by which synapses tuned to similar stimuli arise, especially since recent studies are identifying mechanisms whereby LTP at a strong synapse can facilitate strengthening of a weaker synapse over a spatial domain of up to 15μm[148,149], a similar distance to the distance over which clustering was observed here. Furthermore, the synaptotropic hypothesis suggests that dendritic elaboration, mediated by filopodia extensions, is supported by synapse formation[29]. From this perspective, clustered extensions can be viewed as indicative of an underlying clustering of synapses, supporting the idea that synaptic tuning clustering arises not only in adulthood with experience, but also during dendritogenesis in early development.

Chapter 4: Effects of Acute Excitatory Activity Blockade On Brain Neuron Growth Behavior

4.1 Introduction

A wealth of knowledge exists characterizing the role of activity on growth behavior. Learning has been shown to induce spine formation[132,133,146]. Similarly, artificially stimulating presynaptic neurons has been shown to induce spine formation in the postsynaptic neurons[135]. Eliminating the presynaptic neurons altogether and puffing glutamate onto a stretch of dendrite has been shown to induce spine formation[150]. However, not only dendritic structures are altered. Induction of LTP in neurons is also associated with growth of axonal filopodia and structural changes to axonal varicosities[151,152]. Furthermore, in axons potentiation leads to increased numbers of multi-synapse boutons[153]. Overall, it appears that activity has a role to play in terms of neuronal development and structural plasticity. Interestingly, blockade of activity also can have an effect on neuronal structural plasticity. For example, prolonged infusion of GABA, an inhibitory neurotransmitter, induced the formation of non-innervated postsynaptic membrane thickenings[154]. Blockade of action potentials by applying TTX led to a tripling of spine density of LGN neurons[109]. Although, the literature on the effects of activity blockade also tends to show that neuronal dendritic growth behaviors are not affected by the activity blockade. In one study where all neurotransmitter vesicular release was abolished, the brains of animals looked normal during development[50]. This study suggests that neurons can grow and form connections with other neurons with no excitatory activity at all. One interesting observation is that while activity tends to induce structural plasticity changes on a very rapid timescale, between seconds to tens of minutes, activity blockade tends to induce structural plasticity changes on the scale of days to weeks. To summarize some salient points from the above, it has been shown that neurons can develop their dendritic arbors in the

complete absence of excitatory activity. Furthermore, excitatory activity can induce structural plasticity. Since neurons develop their dendritic arbors by extending filopodia, these observations potentially suggest that two sets of filopodia exist, those that are generated by activity-independent mechanisms and those that are generated by activity-dependent mechanisms. The idea that two sets of filopodia exist was the driving force behind the experiment in this chapter.

In this chapter I conducted an experiment where I used a drug cocktail that acutely blocked all excitatory activity while monitoring structural plasticity at a temporal resolution of 5 minute intervals. This would allow me to suppress the activity-dependent set of filopodia, a change I would be able to identify by monitoring the growth behavior of the neuron.

4.2 Methods

Animal rearing, calcium indicator loading, two-photon imaging and analysis were performed as described in Chapter 2.

4.2.1 Single cell electroporation
In order to get single isolated neurons bright enough for 5 minute imaging for three hours single cell electroporation was used. The technique is described in [126].

4.2.2 Activity blocking cocktail
The cocktail used was designed to block action potential propagation and all glutamatergic receptors, both ionotropic and metabotropic. The cocktail consisted of tetrodotoxin (TTX, 1μM), D-AP5 (50μM), MK-801 (25μM), CNQX (20μM), CGP-52432 (10μM), and LY-341495 (100μM).

4.2.3 Experimental protocol
Visual stimuli were presented via a 635nm LED (LTL-709E, Lite-On Inc.) placed against the eye contralateral to the imaged tectum. Visual stimuli consisted of OFF flashes. An OFF flash is

defined as the LED initially being on and then being turned off for 50ms before being turned on again. Probing consisted of OFF flashes presented once a minute.

The experimental protocol consisted of a baseline of 45 minutes of probing followed by an injection of the activity blocking cocktail, and a further 2 hours of imaging with the LED off. A 3D morphological stack was acquired every 5 minutes throughout, with the exception of the time of injection.

The drug cocktail was administered in two ways. It was injected directly into the tectum and included in the rearing solution. For the injection, the concentrations of the drugs were increased by a factor of 5 (10 for TTX) to account for dilution in the tectum. During perfusion, TTX was excluded since perfusion of the tadpole with TTX increased tadpole mortality. The control consisted of an injection of vehicle without the drug cocktail.

4.3 Results

Majority of growth behaviors were not affected by the administration of the drug cocktail. The morphometric parameters that were examined were dendritic growth behaviors, including filopodia addition, subtraction, extension and retraction rates, filopodia lengths, filopodia survivalship, dendritic arbor length and clustering of growth behaviors.

4.3.1 Activity blocking cocktail blocks action potentials throughout the optic tectum

To test the efficacy of the activity blockade cocktail, spontaneous calcium transients were measured from neuronal somata before and after activity blockade cocktail injection and perfusion. Furthermore, spontaneous activity was assessed in the same population of neurons 24 hours after injection of the drug cocktail.

The drug cocktail blocked the spontaneous activity in 96% of neurons. The blockade persisted for 1.5 hours after the injection. The majority of imaged neurons recovered their activity after 24 hours.

4.3.2 Activity blocking cocktail blocks dendritic activity

While the activity cocktail blocks somatic activity, I was interested in whether the activity blocking cocktail also blocks subthreshold dendritic activity. To answer this question, the dendrites of GCaMP6 expressing neurons were imaged before and after the drug cocktail administration. Additionally, as in the population somatic imaging case the responsiveness of these dendrites was assessed 24 hours after the drug cocktail administration. The drug cocktail blocked 95% of dendritic activity. The blockade persisted for 90 minutes after drug cocktail administration (Fig 4.2). The imaged dendrites were recovered 24 hours later (Fig 4.2).

4.3.3 Injection creates an artifact of decreased filopodia density

In both the control and experimental groups the density of filopodia dropped by a small, yet consistent, amount after the injection. When the projected images of neurons before and after injection were examined, two differences between them could be identified. First, most neurons were slightly rotated in three dimensional space, likely due to tadpole rotation in the chamber during the injection (Fig 4.3). Second, the neurons appeared to be dimmer (Fig 4.3). The decrease in brightness is likely due to the neuron being deeper relative to the skin of the tadpole after the injection, resulting in increased light scattering by the tissue.
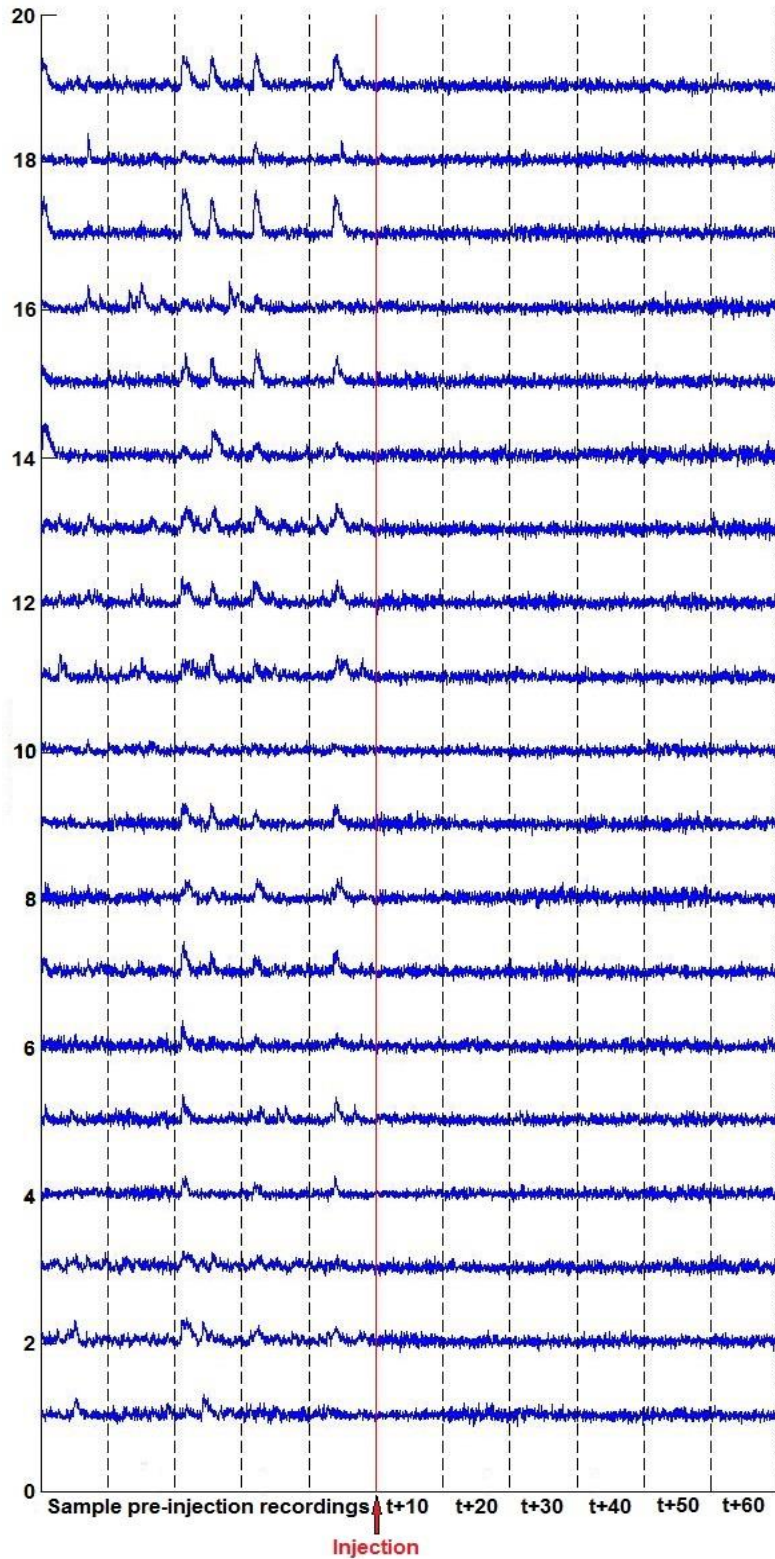
Figure 4.1: Activity blocking cocktail abolishes neuronal spontaneous activity.
Traces of calcium transients in a representative sample of neurons in the optic tectum. Each column, separated by dashed lines, is a 60 second recording of spontaneous activity of these neurons. Before the injection 5 such recordings are presented as a baseline. After the injection recordings were acquired every 10 minutes.
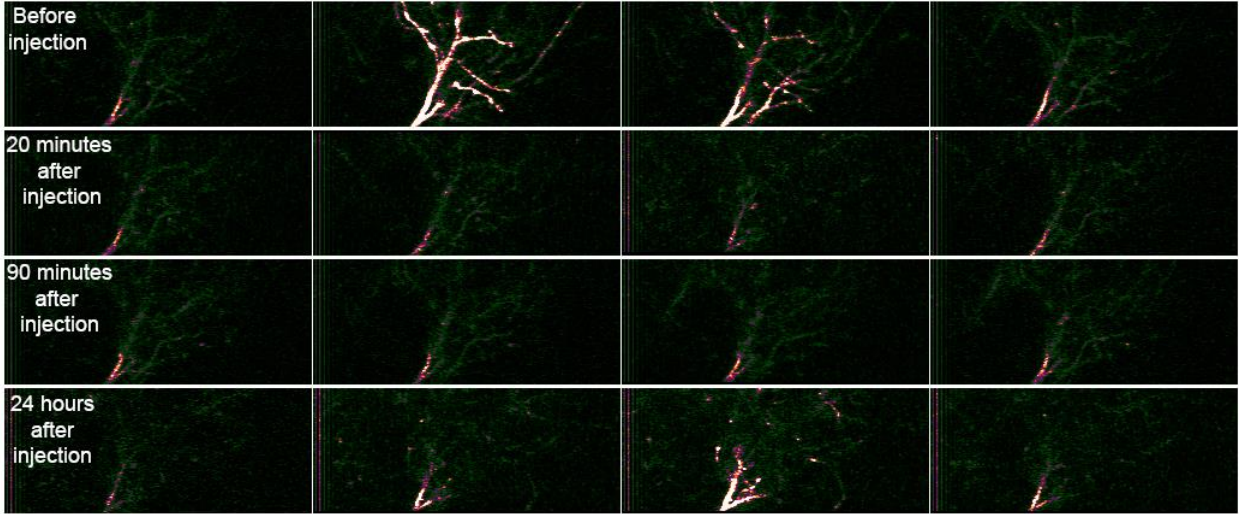
Figure 4.2: Activity blocking cocktail blocks dendritic calcium transients.
A representative series of images showing spontaneous dendritic activity before, shortly after and after recovery from the injection of the activity blocking cocktail.
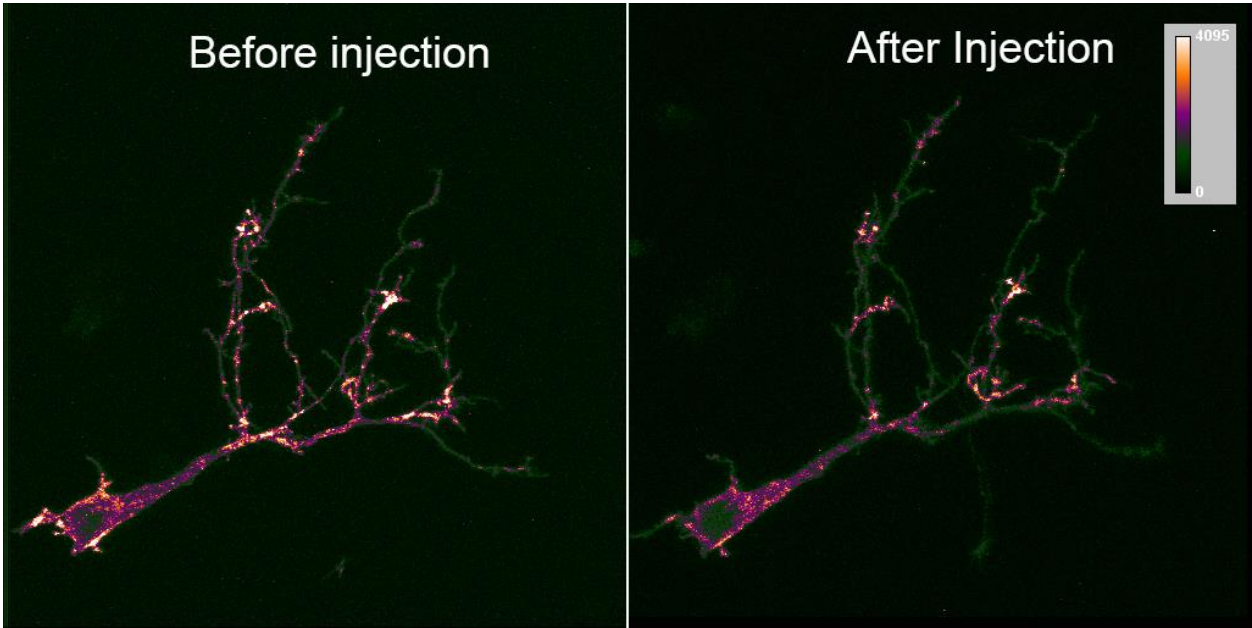
Figure 4.3: Effects of an injection on neurons.
A representative example of the rotation and dimming of a neuron after injection.
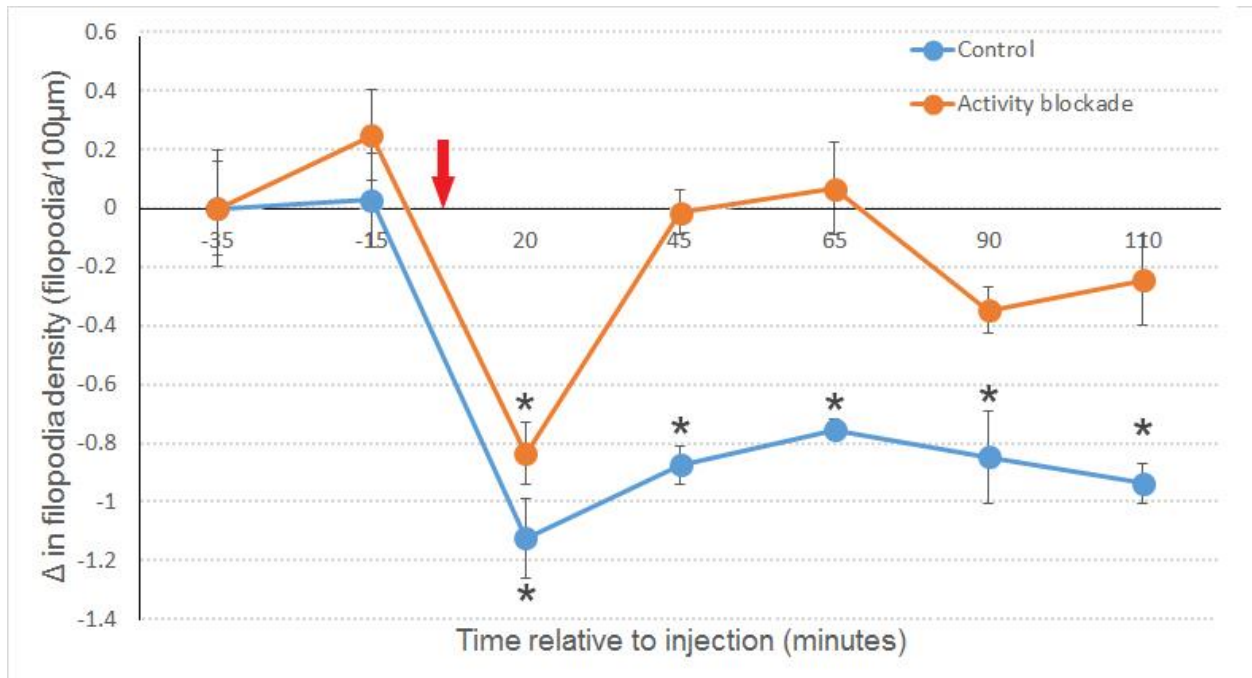
Figure 4.4: Effects of activity blockade on filopodia density.
Mean rate of change in filopodia density over time, binned over 20 minutes per data point. Rates are expressed as the mean filopodia density minus the mean filopodia density at time -35 min. Red arrow indicates the time of injection. N = 4 (Control); 4 (Activity blockade). *p<0.01 relative to filopodia density at time -35 min. Error bars are SE. Statistics were done with a one way ANOVA followed by the Tukey-Kramer post hoc test for each experimental condition.
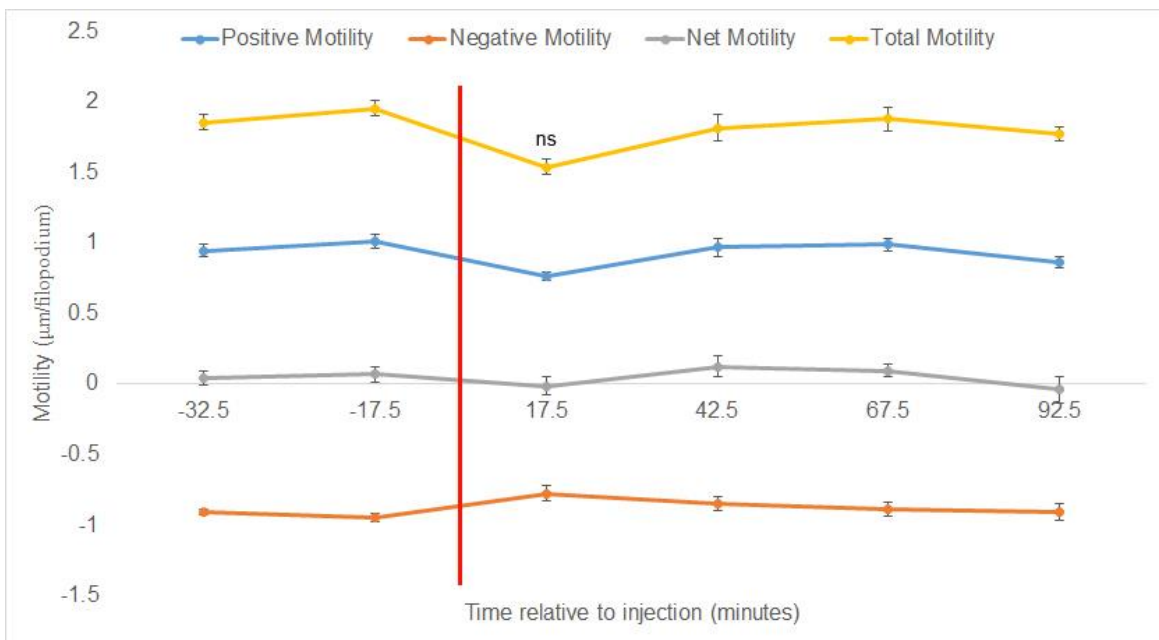
Figure 4.5: Activity blockade does not change filopodia motility.
Mean filopodia motility rate over time, binned over 20 minutes per data point. Red vertical line represents the time of injection. Net motility is positive motility + negative motility, and total motility is positive motility + absolute negative motility. Error bars are SE. Statistics are done with a one way ANOVA followed by the Tukey-Kramer post hoc test.
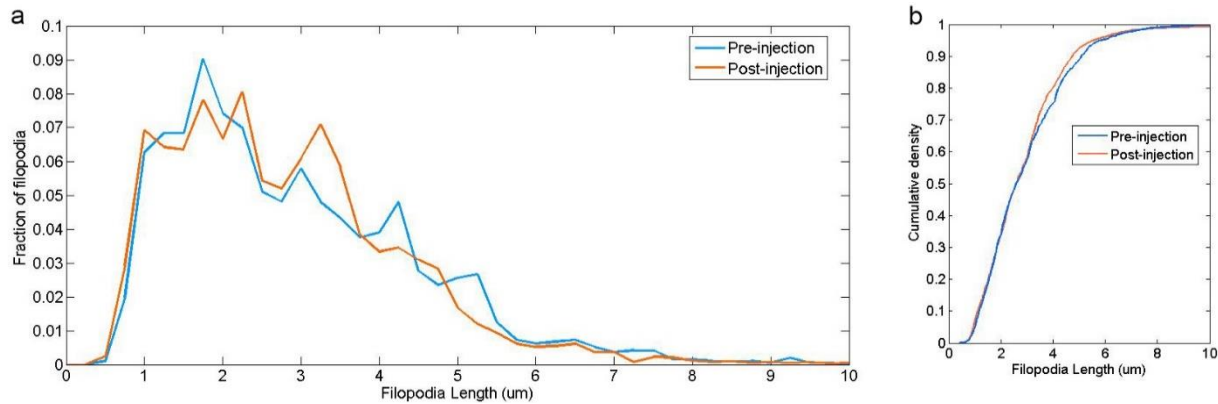
Figure 4.6: Activity blockade does not change filopodia lengths.
All filopodial lengths were measured at each time-point. N = 1917 (pre-injection), 4410 (post-injection) in 4 neurons. **a)** Distribution of filopodia lengths before and after the injection. **b)** Empirical cumulative density function. For statistics a two-sample Kolgomorov-Smirnoff test was used.
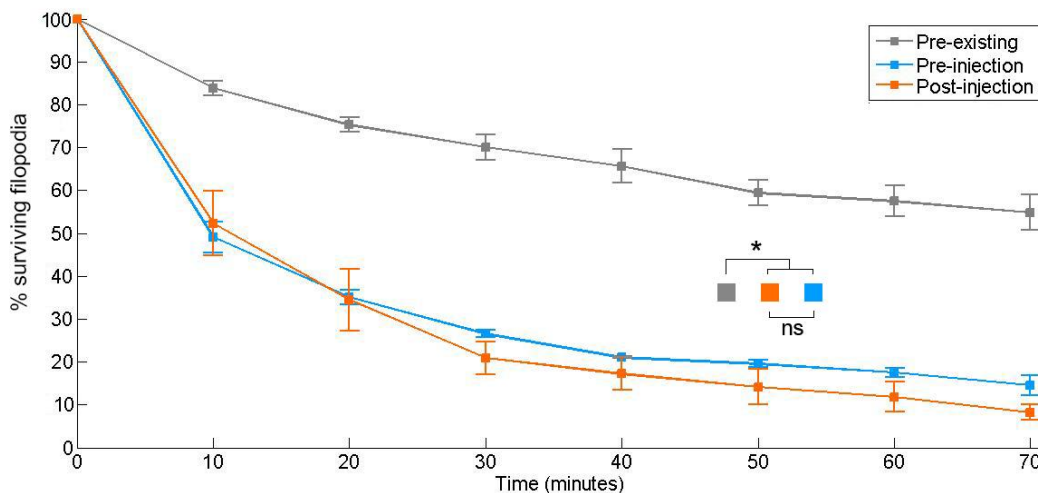
Figure 4.7: Activity blockade does not affect filopodia survivalship.
The fraction of filopodia surviving up to a given length of time. Only filopodia born up to 40 minutes after the injection are considered in the post-injection group. N = 1917 (pre-injection), 1754 (post-injection) in 4 neurons. Error bars are SE. * p < 0.01. Survivalship was compared using a two sample Kolgomorov-Smirnoff test with Bonferroni correction for multiple tests.

4.3.4 Activity blocking cocktail increases filopodia density

In both the control and experimental groups filopodia density decreased in the first 10 minutes after injection (Fig 4.4). This observation is described further in the previous section. Focusing on the density after the injection, in the control group density is maintained for the duration of the

experiment. However, when in the presence of the activity blockade cocktail, filopodial density increases 30 minutes after the injection and remains stable for the rest of the experiment.

4.3.5 Activity blockade did not alter filopodia motility, length or survivalship

The motility of filopodia, namely the extension or retraction of filopodia, was not altered by the activity blockade (Fig. 4.5). Similarly, the lengths of filopodia before and after the activity blockade had the same distribution (Fig. 4.6). Furthermore, while pre-existing filopodia survived longer than new filopodia, of the filopodia that appeared during imaging the survivalship of filopodia born before and after activity blockade was similar (Fig. 4.7). The dendritic arbor length remained unchanged throughout the experiment.

4.3.6 Activity blockade does not affect clustering of growth behaviors

Examination of distances between closest filopodia exhibiting the same growth behavior can be used to assess clustering of the growth behaviors. Here, the distribution of distances are for each growth behavior is determined and compared to the distribution that is expected by chance. To determine the expected distribution for each neuron all the filopodia were removed from the dendritic tree and randomly places back onto the dendritic tree. In addition, each filopodium was then randomly assigned a growth behavior from the set of growth behaviors that were found on the original neuron. This randomization process was done 10 times for each neuron at each time-point. Clustering was not observed for any growth behavior before or after activity blockade (Fig. 4.7).
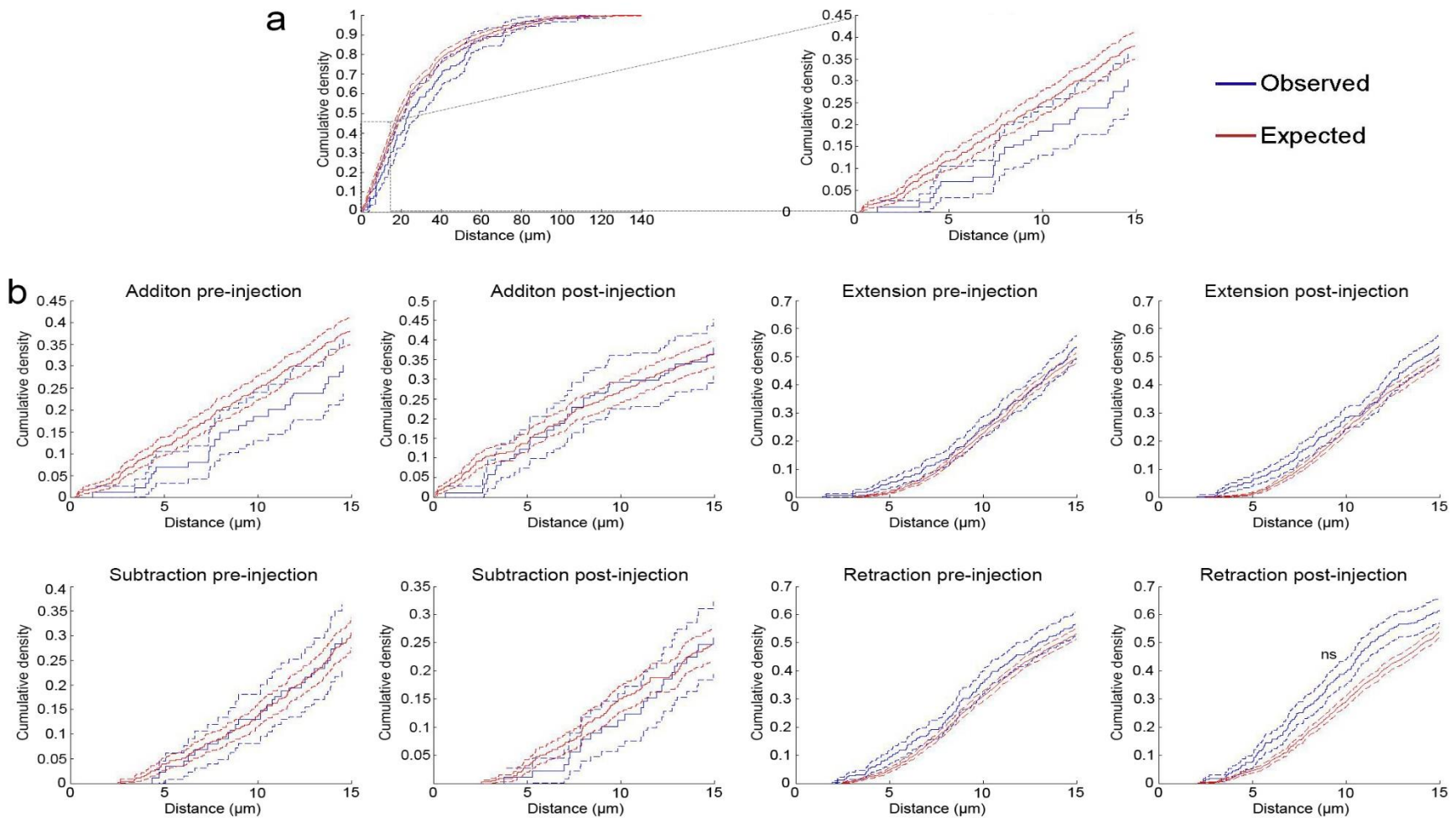
Figure 4.7: Clustering of different growth behaviors before and after activity blockade.
Cumulative densities of distances between a filopodium of a specified growth behavior to the closest filopodium of the same growth behavior. *Expected* densities were derived by randomly rearranging all filopodia on the tree and then randomly assigning the growth behavior labels found on the original tree. Each *expected* cumulative density is a combination of 10 randomizations. **a)** Shows how the panels in **b** were created. **b)** Sections of cumulative densities for distances up to 15μm for growth behaviors before and after injection of activity blocking cocktail. Pre-injection N = 176 (additions), 189 (subtractions), 524 (retractions), 578 (extensions); Post-injection N = 178 (additions), 171 (subtractions), 459 (retractions), 540 (extensions) in 4 neurons. Error bars are SE. Statistical significance was tested using the Kolmogorov-Smirnoff test.

55

4.4 Discussion

For the work in this chapter all excitatory activity was blocked using a drug cocktail that was administered into the optic tectum of *Xenopus laevis* tadpoles. The growth of phase 2 neurons was assessed for 45 minutes before and for 95 minutes after activity blockade. Nearly all morphometric parameters remained unchanged by the activity blockade. Many studies investigating the effects of activity blockade on growth behaviors observe that structural plasticity occurs on a time scale of days to weeks[109,154], while in this experiment short-term structural plasticity was monitored over less than 2 hours after activity blockade. The specific morphometric parameters and their behavior with activity blockade are discussed below.

4.4.1 Filopodia addition rate remained unaltered by activity blockade

Evidence exists for activity-driven growth of dendritic protrusions[132,133,135,146,150]. Due to this, activity blockade was expected to lower the addition rate upon administration of the drug cocktail, however, no such change was observed. The lack of change in the addition rate could be for three reasons.

First, there could have been no activity-dependent filopodia additions occurring. The data collected in this experiment cannot exclude this possibility. However, given the work in the previous chapter, the literature on activity-dependent growth dynamics in tectal neurons and the work on the synaptotropic hypothesis this possibility is unlikely.

Second, the activity-dependent addition rate may have been suppressed but the rate was small in comparison to the activity-independent rate and was thus not seen. To examine this idea further it is pertinent to point out that phase 2 neurons were used in this experiment. Phase 2 neurons tend to exhibit high levels of growth behaviors as these neurons are in the process of rapid dendritic arbor elaboration[9,10]. The thought was that any changes to growth behaviors would be more easily

identified on a more active background of growth behaviors. Furthermore, the synaptotropic hypothesis suggests that much of the dendritic development will be guided by active, relevant contacts. However, since these neurons are expanding their arbors rapidly it is possible that general seeking behavior dominates at this stage of development. Moreover, it is possible that at this stage of neuronal development it would be counterproductive for neurons to specialize excessively into a single circuit as this could result in hyper-stabilization before maturation of the dendritic arbor and this would make it difficult for the neuron to establish connections with other circuits to allow for specialization in other circuits if they became more relevant at a later time. If this is the case, using phase 3 neurons, with stable established dendritic arbors that nevertheless show structural plasticity, may help expose an effect on growth behaviors since the activity-independent growth will likely be reduced.

Third, since the injection precluded imaging, and as a result the first structural plasticity measure was not available until 15 minutes after the start of the activity blockade, the activity-dependent rate may have been suppressed and compensated for without being observed. While 15 minutes is a very short amount of time for compensation to occur, this possibility is included here for the sake of completeness.

4.4.2 Activity blockade did not alter filopodia stability

The lifetimes of new filopodia were unaltered with the activity blockade. Some studies show that activity stabilizes filopodia[30,104–106] and thus it could be expected that activity blockade would have a destabilizing effect on filopodia. One explanation is that filopodia are stabilized initially by trans-synaptic cell adhesion molecules (CAMs), which when inhibited decrease filopodial lifetimes[51]. Since CAMs were not affected by the activity blockade, similar filopodia stability of nascent filopodia before and after activity blockade is not surprising. However, with activity blockade the

nascent filopodia were expected to not be stabilized by activity and thus have a shorter lifetime beyond the initial stages mediated by CAMs. This is perhaps the case, however the majority of filopodia before and after activity blockade did not become stabilized, potentially masking any differences in activity-dependent filopodia stabilization that could have occurred. This conclusion is supported by the trend that filopodia born after the activity blockade have a slightly lower, and not statistically significant, survivalship for times beyond 30 minutes.

The pre-existing filopodia maintain a steady and consistent survivalship profile with a linearly smaller fraction of filopodia surviving for a longer time frame. Interestingly, a sharp decrease is not seen in these filopodia after the activity is blocked. This is likely because for a filopodium to retract past a synapse, the synapse must be dissolved[29], but some studies indicate that LTD is dependent on NMDA receptors[155,156], which were blocked with activity blockade potentially preserving the filopodia that had established synapses. This line of reasoning can also be applied to the observed trend that filopodia born before activity blockade have a marginally higher survivalship, since some of these filopodia would likely have established synapses before the activity blockade.

4.4.3 Clustering of growth behaviors is absent before and after activity blockade

An interesting aspect of the results from the work in this chapter is that no clustering of growth behaviors was observed, before or after activity blockade. It is established that activity drives clustering of synapses with similar tuning[133,147] and the work in chapter 3 suggests that the clustering of additions and extensions can potentially be a mechanism by which such clustering of tuning properties arises. However, clustering was not observed even before activity blockade. There are two explanations that could account for this observation. First, unlike the work in chapter 3 where morphology was assessed for changes every 30 minutes, here morphology was assessed

every 5 minutes. This suggests that perhaps it is clustering of additions that are stable over a longer time-frame that are important for tuning clustering rather than short-term growth behavior. This conclusion is supported both by literature that describes inter-synapse plasticity mechanisms where a strong synapse can aid a weaker synapse to potentiate over a short distance[148,149] and by the observation that extensions, which are often supported by synapses, were clustered in the work in chapter 3 since synapses are found to support filopodial extension[10,29]. Second, the neurons used for this experiment are young and in the process of elaborating their dendritic arbor. Thus, it is possible that a large fraction of their growth behaviors are not guided by activity, which masks any activity-driven clustering that may be occurring.

4.4.4 Changes in filopodia density

In terms of morphometrics that showed altered behavior, it is surprising that when vehicle or vehicle with the drug cocktail were injected filopodia density decreased. This suggests that the injection may be causing some change in the neurons. This change may be damage to the neurons in the tectum or an artifact of the tectal expansion and rotation of the tadpole in the chamber resulting in a different perspective of the neuron when imaged. Furthermore, neurons tended to decrease in brightness, possibly due to expansion of the tectum above the neuron introducing increased light scattering, after injection. Upon examining projections of neurons before and after injection the more likely option is that the decrease in filopodia density is an artifact of rotation and decrease in brightness due to increased light scattering.

When the decrease in density is seen as an artifact of the injection, the results suggest that while activity blockade does not change addition and subtraction rates significantly, compensation occurs 30 minutes after the onset of the blockade that increases filopodia density. An increase in density in response to activity blockade has previously been observed, also without a change in

growth behaviors, although in that experiment activity blockade lasted two weeks before the researchers examined the neurons for changes[109]. A compensatory increase in density is a reasonable response for a neuron that lost activity since it would attempt to find connections that are not silent. The timing of 30 minutes suggests that this change could be a result of transcriptional changes, hinting at either a mechanistic link between the activity-dependent and activity-independent filopodia generation mechanisms or a global measure of activity that controls the rate of activity-independent filopodia formation.

4.4.5 Role of competition

One aspect of this experimental design that should be discussed is that in this experiment activity blockade was administered to the entire tectum, rather to an individual neuron. As a result, the competition for axons was not altered. No neuron was at an advantage or disadvantage to any other neuron. In such a system, it is reasonable to expect that growth behaviors would not change, since a critical driving force of dendritic expansion, competition, remained functionally unaltered. Blocking the activity of all neurons is common in the activity blockade literature since it makes experimental setup much simpler. However, blocking activity in a single neuron while monitoring structural plasticity would be an interesting avenue of research to pursue, especially since some studies show that AMPA receptor blockade in a single neuron results in simpler dendritic arbors with longer primary branches, suggesting that competition is critical to structural plasticity[30].

Chapter 5: Conclusion

5.1 Summary of findings

For this thesis my objectives were as follows:

1: To develop and optimize methods for transfecting single neurons in vivo based on the neurons functional characteristics.

2: To determine the relationship between dendritic arbor growth and functional plasticity during refinement.

3: To characterize activity-dependent and –independent dendritogenesis.

By loading the optic tectum with a calcium indicator such as Oregon Green Bapta 1 – AM and then observing calcium transients under a two-photon microscope it is possible to visualize action potential firing of neurons. Coupling this capability with visual stimuli allows for identification of neurons that respond to a specific known stimulus. Furthermore, chapter 2 also demonstrates how to reliably transfect a single neuron with macromolecules, including plasmid DNA, in a region of densely packed neuronal somata. Overall, chapter 2 describes a method that can be used to reliably introduce macromolecules into neurons based on their functional properties.

Chapter 3 uses the method described in chapter 2 in order to study neurons that respond to a specific visual stimulus, in this case an OFF flash. Here, neurons were trained with an LTP inducing spaced training protocol in order to elucidate the relationship between functional and structural plasticity. Both neurons that were responsive and not responsive to the stimulus showed unique growth patterns when trained. Responsive neurons tended to prune in response to training while non-responsive neurons tended to expand their arbors. Interestingly, some neurons acquired

a response with training. These neurons resembled non-responding neurons before acquiring a response in that they expanded their dendritic arbor. However, after acquiring a response these neurons resembled responsive neurons and pruned their arbors. All of the observed training induced growth behaviors required NMDA receptors.

Chapter 4 focused on characterizing activity-dependent and activity-independent dendritogenesis. This was achieved by introducing a drug cocktail that inhibited all excitatory activity in the optic tectum while monitoring the growth behavior of a young neuron. The work in this chapter suggests that filopodia generation of young neurons is primarily driven by activity independent mechanisms since the addition and subtraction rates of filopodia did not change when excitatory activity was abolished. However, activity does appear to play a role in early dendritogenesis since 30 minutes after excitatory activity blockade filopodia density increased, suggesting that compensation is occurring.

5.2 Future directions

5.2.1 Role of calcium in activity-driven growth behavior

Chapter 3 presents evidence for activity-driven modifications to dendritic growth behavior that is associated with functional plasticity of the neuronal output. The neuronal output is a consequence of integration of synaptic input from across the arbor[17,18]. Thus, it is likely the plastic changes to synapses across the dendritic arbor that underlie the somatic changes observed. Furthermore, synaptic plasticity is known to influence local dendritic growth behavior[106,134,135,145]. Some studies suggest that calcium plays a role in regulating growth behaviors of the local dendritic arbor[44,47–49]. Other studies suggest that global calcium dynamics can have an effect on transcription-factor mediated dendritic growth[49]. With technology that allows ultrafast imaging of three dimensional space[157,158] coupled with genetically expressed calcium indicators[159] it is now possible to image

the calcium dynamics across the entire arbor at the same time. Doing this would allow the integration of the existing knowledge of local and global effects of calcium on dendritic growth into a comprehensive understanding of why neurons alter their dendritic growth behavior in stereotypical ways.

5.2.2 Role of transcription factors in activity-driven growth behavior

Some studies suggest that transcriptional factors are involved in the regulation of dendritic growth behaviors[49,75,160,161]. The work in chapter 3 suggests that transcription factors may be involved in the observed results based on the timing of growth behaviors. A delay in onset of behavioral changes was observed in some instances suggesting the involvement of transcription factors. In order to further understand the range of growth behaviors seen it would be interesting to study the effects of a battery of blockades, starting with a general blockade of transcription and if an effect on the growth behavior is observed continue by identifying the specific transcription factor by more targeted blockades. Some candidate transcription factors that could be focused on are the calcium dependent CREST and NeuroD[75,160]. Another option could be MEF2 since the difference between the growth patterns of the activity profiles could be influenced by metaplasticity mechanisms[137].

5.2.3 Neuronal maturation-dependent role of activity in dendritogenesis

Research supporting the synaptotropic hypothesis shows that activity is a critical component of dendritogenesis. However, the activity-blockade research shows that dendritogenesis can occur without activity. One way to reconcile these findings is that dendritogenesis occurs by both activity-dependent and activity-independent mechanisms simultaneously. In chapter 4, I show that in immature phase 2 neurons excitatory activity blockade does not clearly separate the filopodia that are generated by the two mechanisms. One explanation is that the activity-independent

mechanism dominates at this early stage of neuronal development. It would be interesting to see if more mature neurons have a larger activity-dependent filopodia generation rate compared to more immature neurons. This would provide insight into how the fine structure of a neuron is formed throughout development. Furthermore, molecular mechanisms underlying each type of dendritic growth could then begin to be explored by identifying differences of gene expression at the different maturation stages.

5.3 Significance

While single cell electroporation was developed in the optic tectum of *Xenopus laevis* tadpoles[126] the majority of targeted single-cell electroporation development *in vivo* has focused on rodents[130,162,163]. However, in the amphibian optic tectum neuronal somata are much more densely packed posing a challenge when attempting to use the targeted single-cell electroporation technique. In this thesis I have developed a protocol for reliably transfecting single neurons using targeted single cell electroporation in a region of densely packed neuronal somata. Furthermore, in chapter 2 I describe a method for selecting neurons based on their tuning, which I implement in chapter 3. The neuronal tuning to sensory stimuli is a critical criterion for neuronal selection in the study of activity-dependent dendritic growth as can be seen in chapter 3. However, many studies do not take this factor into account when examining activity-dependent dendritic growth[106,132,133]. The work in this thesis highlights that neuronal tuning should be considered when selecting neurons for activity-dependent dendritic growth studies and provides a method that will allow researchers to accomplish this type of neuronal selection.

Chapters 3 and 4 of this thesis contribute to the field of activity-dependent dendritogenesis by demonstrating that neurons grow in stereotypical growth patterns in response to circuit activation. The specific growth patterns are likely rooted in the local synapse influences over dendritic growth

behavior, however, the work done here suggests that a shift in perspective from individual synapses and branches to the entire dendritic arbor could reveal more general mechanisms of dendritic growth control. This was especially evident in the activity blockade portion in chapter 4 where activity blockade did not alter the growth dynamics by a discernable degree but caused a compensatory increase in filopodia density.

References

1. Kaufmann, W. E. & Moser, H. W. Dendritic anomalies in disorders associated with mental retardation. *Cereb. Cortex* **10,** 981–991 (2000).

2. Pardo, C. A. & Eberhart, C. G. The neurobiology of autism. *Brain Pathol.* **17,** 434–447 (2007).

3. Walsh, C. A., Morrow, E. M. & Rubenstein, J. L. Autism and brain development. *Cell* **135,** 396–400 (2008).

4. Kelleher, R. J. & Bear, M. F. The autistic neuron: troubled translation? *Cell* **135,** 401–406 (2008).

5. Bagni, C. & Greenough, W. T. From mRNP trafficking to spine dysmorphogenesis: the roots of fragile X syndrome. *Nat. Rev. Neurosci.* **6,** 376–387 (2005).

6. Ramocki, M. B. & Zoghbi, H. Y. Failure of neuronal homeostasis results in common neuropsychiatric phenotypes. *Nature* **455,** 912–918 (2008).

7. Dindot, S. V., Antalffy, B. A., Bhattacharjee, M. B. & Beaudet, A. L. The Angelman syndrome ubiquitin ligase localizes to the synapse and nucleus, and maternal deficiency results in abnormal dendritic spine morphology. *Hum. Mol. Genet.* **17,** 111–118 (2008).

8. Garey, L. J. *et al.* Reduced dendritic spine density on cerebral cortical pyramidal neurons in schizophrenia. *J. Neurol. Neurosurg. Psychiatry* **65,** 446–453 (1998).

9. Wu, G. Y., Zou, D. J., Rajan, I. & Cline, H. Dendritic dynamics in vivo change during neuronal maturation. *J. Neurosci.* **19,** 4472–4483 (1999).

10. Hossain, S., Sesath Hewapathirane, D. & Haas, K. Dynamic morphometrics reveals contributions of dendritic growth cones and filopodia to dendritogenesis in the intact and awake embryonic brain. *Dev. Neurobiol.* **72,** 615–627 (2012).

11. Wong, W. T. & Wong, R. O. Rapid dendritic movements during synapse formation and rearrangement. *Curr. Opin. Neurobiol.* **10,** 118–124 (2000).

12. Bray, D. Branching patterns of individual sympathetic neurons in culture. *J. Cell Biol.* **56,** 702–712 (1973).

13. Bartlett, W. P. & Banker, G. A. An electron microscopic study of the development of axons and dendrites by hippocampal neurons in culture. I. Cells which develop without intercellular contacts. *J. Neurosci.* **4,** 1944–1953 (1984).

14. Bartlett, W. P. & Banker, G. A. An electron microscopic study of the development of axons and dendrites by hippocampal neurons in culture. II. Synaptic relationships. *J. Neurosci.* **4,** 1954–1965 (1984).

15. Craig, A. M. & Banker, G. Neuronal polarity. *Annu. Rev. Neurosci.* **17,** 267–310 (1994).

16. Yuste, R. & Tank, D. W. Dendritic integration in mammalian neurons, a century after Cajal. *Neuron* **16,** 701–716 (1996).

17. Magee, J. C. Dendritic integration of excitatory synaptic input. *Nat. Rev. Neurosci.* **1,** 181–190 (2000).

18. Stuart, G. J. & Spruston, N. Dendritic integration: 60 years of progress. *Nat. Neurosci.* **18,** 1713–1721 (2015).

19. Baas, P. W., Deitch, J. S., Black, M. M. & Banker, G. A. Polarity orientation of microtubules in hippocampal neurons: uniformity in the axon and nonuniformity in the dendrite. *Proc. Natl. Acad. Sci.* **85,** 8335–8339 (1988).

20. Heidemann, S. R., Landers, J. M. & Hamborg, M. A. Polarity orientation of axonal microtubules. *J. Cell Biol.* **91,** 661–665 (1981).

21. Horton, A. C. *et al.* Polarized secretory trafficking directs cargo for asymmetric dendrite growth and morphogenesis. *Neuron* **48,** 757–771 (2005).

22. Kosik, K. S. & Finch, E. A. MAP2 and tau segregate into dendritic and axonal domains after the elaboration of morphologically distinct neurites: an immunocytochemical study of cultured rat cerebrum. *J. Neurosci.* **7,** 3142–3153 (1987).

23. Sharp, D. J. *et al.* Identification of a microtubule-associated motor protein essential for dendritic differentiation. *J. Cell Biol.* **138,** 833–843 (1997).

24. Goslin, K., Schreyer, D. J., Skene, J. P. & Banker, G. Development of neuronal polarity: GAP-43 distinguishes axonal from dendritic growth cones. *Nature* **336,** 672–674 (1988).

25. McAllister, A. K. Cellular and molecular mechanisms of dendrite growth. *Cereb. Cortex* **10,** 963–973 (2000).

26. Cline, H. T. Dendritic arbor development and synaptogenesis. *Curr. Opin. Neurobiol.* **11,** 118–126 (2001).

27. Wong, R. O. & Ghosh, A. Activity-dependent regulation of dendritic growth and patterning. *Nat. Rev. Neurosci.* **3,** 803–812 (2002).

28. Jontes, J. D., Buchanan, J. & Smith, S. J. Growth cone and dendrite dynamics in zebrafish embryos: early events in synaptogenesis imaged in vivo. *Nat. Neurosci.* **3,** 231–237 (2000).

29. Niell, C. M., Meyer, M. P. & Smith, S. J. In vivo imaging of synapse formation on a growing dendritic arbor. *Nat. Neurosci.* **7,** 254–260 (2004).

30. Haas, K., Li, J. & Cline, H. T. AMPA receptors regulate experience-dependent dendritic arbor growth invivo. *Proc. Natl. Acad. Sci.* **103,** 12127–12131 (2006).

31. Rall, W. DISTINGUISHING THEORETICAL SYNAPTIC POTEN-TIALS COMPUTED FOR DIFFERENT SOMA-DEN-DRITIC DISTRIBUTIONS OF SYNAPTIC INPUT. (1967).

32. Spruston, N., Jaffe, D. B. & Johnston, D. Dendritic attenuation of synaptic potentials and currents: the role of passive membrane properties. *Trends Neurosci.* **17,** 161–166 (1994).

33. Golding, N. L., Mickus, T. J., Katz, Y., Kath, W. L. & Spruston, N. Factors mediating powerful voltage attenuation along CA1 pyramidal neuron dendrites. *J. Physiol.* **568,** 69–82 (2005).

34. Stuart, G. & Spruston, N. Determinants of voltage attenuation in neocortical pyramidal neuron dendrites. *J. Neurosci.* **18,** 3501–3510 (1998).

35. Johnston, D., Magee, J. C., Colbert, C. M. & Christie, B. R. Active properties of neuronal dendrites. *Annu. Rev. Neurosci.* **19,** 165–186 (1996).

36. Polsky, A., Mel, B. & Schiller, J. Encoding and decoding bursts by NMDA spikes in basal dendrites of layer 5 pyramidal neurons. *J. Neurosci* **29,** 11891–11903 (2009).

37. Schiller, J., Major, G., Koester, H. J. & Schiller, Y. NMDA spikes in basal dendrites of cortical pyramidal neurons. *Nature* **404,** 285–289 (2000).

38. Yuste, R., Gutnick, M. J., Saar, D., Delaney, K. R. & Tank, D. W. Ca 2+ accumulations in dendrites of neocortical pyramidal neurons: an apical band and evidence for two functional compartments. *Neuron* **13,** 23–43 (1994).

39. Vaughn, J. E. Review: fine structure of synaptogenesis in the vertebrate central nervous system. *Synapse* **3,** 255–285 (1989).

40. Vaughn, J. E., Henrikson, C. K. & Grieshaber, J. A. A quantitative study of synapses on motor neuron dendritic growth cones in developing mouse spinal cord. *J. Cell Biol.* **60,** 664–672 (1974).

41. Vaughn, J. E., Barber, R. P. & Sims, T. J. Dendritic development and preferential growth into synaptogenic fields: A quantitative study of Golgi-impregnated spinal motor neurons. *Synapse* **2,** 69–78 (1988).

42. Cline, H. & Haas, K. The regulation of dendritic arbor development and plasticity by glutamatergic synaptic input: a review of the synaptotrophic hypothesis. *J. Physiol.* **586,** 1509–1517 (2008).

43. Chen, S. X. & Haas, K. Function directs form of neuronal architecture. *Bioarchitecture* **1,** 2–4 (2011).

44. Wu, G.-Y. & Cline, H. T. Stabilization of dendritic arbor structure in vivo by CaMKII. *Science* **279,** 222–226 (1998).

45. Keuren-Jensen, V., Kendall, R. & Cline, H. T. Homer proteins shape Xenopus optic tectal cell dendritic arbor development in vivo. *Dev. Neurobiol.* **68,** 1315–1324 (2008).

46. Liu, X. F., Tari, P. K. & Haas, K. PKMζ restricts dendritic arbor growth by filopodial and branch stabilization within the intact and awake developing brain. *J. Neurosci.* **29,** 12229–12235 (2009).

47. Lohmann, C., Myhr, K. L. & Wong, R. O. Transmitter-evoked local calcium release stabilizes developing dendrites. *Nature* **418,** 177–181 (2002).

48. Lohmann, C., Finski, A. & Bonhoeffer, T. Local calcium transients regulate the spontaneous motility of dendritic filopodia. *Nat. Neurosci.* **8,** 305–312 (2005).

49. Lohmann, C. & Wong, R. O. Regulation of dendritic growth and plasticity by local and global calcium dynamics. *Cell Calcium* **37,** 403–409 (2005).

50. Verhage, M. *et al.* Synaptic assembly of the brain in the absence of neurotransmitter secretion. *Science* **287,** 864–869 (2000).

51. Chen, S. X., Tari, P. K., She, K. & Haas, K. Neurexin-neuroligin cell adhesion complexes contribute to synaptotropic dendritogenesis via growth stabilization mechanisms in vivo. *Neuron* **67,** 967–983 (2010).

52. Siddiqui, T. J. & Craig, A. M. Synaptic organizing complexes. *Curr. Opin. Neurobiol.* **21,** 132–143 (2011).

53. Craig, A. M. & Kang, Y. Neurexin–neuroligin signaling in synapse development. *Curr. Opin. Neurobiol.* **17,** 43–52 (2007).

54. Bamji, S. X. Cadherins: actin with the cytoskeleton to form synapses. *Neuron* **47,** 175–178 (2005).

55. Dalva, M. B., McClelland, A. C. & Kayser, M. S. Cell adhesion molecules: signalling functions at the synapse. *Nat. Rev. Neurosci.* **8,** 206–220 (2007).

56. Scheiffele, P., Fan, J., Choih, J., Fetter, R. & Serafini, T. Neuroligin expressed in nonneuronal cells triggers presynaptic development in contacting axons. *Cell* **101,** 657–669 (2000).

57. Lise, M. F. & El-Husseini, A. The neuroligin and neurexin families: from structure to function at the synapse. *Cell. Mol. Life Sci. CMLS* **63,** 1833–1849 (2006).

58. Irie, M. *et al.* Binding of neuroligins to PSD-95. *Science* **277,** 1511–1515 (1997).

59. Graf, E. R., Zhang, X., Jin, S.-X., Linhoff, M. W. & Craig, A. M. Neurexins induce differentiation of GABA and glutamate postsynaptic specializations via neuroligins. *Cell* **119,** 1013–1026 (2004).

60. Liao, D., Hessler, N. A. & Malinow, R. Activation of postsynaptically silent synapses during pairing-induced LTP in CA1 region of hippocampal slice. (1995).

61. Isaac, J. T., Crair, M. C., Nicoll, R. A. & Malenka, R. C. Silent synapses during development of thalamocortical inputs. *Neuron* **18,** 269–280 (1997).

62. Wu, G.-Y., Malinow, R. & Cline, H. T. Maturation of a central glutamatergic synapse. *Science* **274,** 972 (1996).

63. Williams, K., Russell, S. L., Shen, Y. M. & Molinoff, P. B. Developmental switch in the expression of NMDA receptors occurs in vivo and in vitro. *Neuron* **10,** 267–278 (1993).

64. Shi, S.-H. *et al.* Rapid spine delivery and redistribution of AMPA receptors after synaptic NMDA receptor activation. *Science* **284,** 1811–1816 (1999).

65. Bliss, T. V. & Lømo, T. Long-lasting potentiation of synaptic transmission in the dentate area of the anaesthetized rabbit following stimulation of the perforant path. *J. Physiol.* **232,** 331–356 (1973).

66. Citri, A. & Malenka, R. C. Synaptic plasticity: multiple forms, functions, and mechanisms. *Neuropsychopharmacology* **33,** 18–41 (2008).

67. Lazar, G. Y. The development of the optic tectum in Xenopus laevis: a Golgi study. *J. Anat.* **116,** 347 (1973).

68. Grueber, W. B., Jan, L. Y. & Jan, Y. N. Tiling of the Drosophila epidermis by multidendritic sensory neurons. *Development* **129,** 2867–2878 (2002).

69. Parrish, J. Z., Kim, M. D., Jan, L. Y. & Jan, Y. N. Genome-wide analyses identify transcription factors required for proper morphogenesis of Drosophila sensory neuron dendrites. *Genes Dev.* **20,** 820–835 (2006).

70. Grueber, W. B., Jan, L. Y. & Jan, Y. N. Different levels of the homeodomain protein cut regulate distinct dendrite branching patterns of Drosophila multidendritic neurons. *Cell* **112,** 805–818 (2003).

71. Li, W., Wang, F., Menut, L. & Gao, F.-B. BTB/POZ-zinc finger protein abrupt suppresses dendritic branching in a neuronal subtype-specific and dosage-dependent manner. *Neuron* **43,** 823–834 (2004).

72. Sugimura, K., Satoh, D., Estes, P., Crews, S. & Uemura, T. Development of morphological diversity of dendrites in Drosophila by the BTB-zinc finger protein abrupt. *Neuron* **43,** 809–822 (2004).

73. Kim, M. D., Jan, L. Y. & Jan, Y. N. The bHLH-PAS protein Spineless is necessary for the diversification of dendrite morphology of Drosophila dendritic arborization neurons. *Genes Dev.* **20,** 2806–2819 (2006).

74. Moore, J. H., Hahn, L. W., Ritchie, M. D., Thornton, T. A. & White, B. C. Application of genetic algorithms to the discovery of complex models for simulation studies in human genetics. in *Proceedings of the Genetic and Evolutionary Computation Conference/GECCO. Genetic and Evolutionary Computation Conference* **2002,** 1150 (NIH Public Access, 2002).

75. Aizawa, H. *et al.* Dendrite development regulated by CREST, a calcium-regulated transcriptional activator. *Science* **303,** 197–202 (2004).

76. Hand, R. *et al.* Phosphorylation of Neurogenin2 specifies the migration properties and the dendritic morphology of pyramidal neurons in the neocortex. *Neuron* **48,** 45–62 (2005).

77. Bentley, D. & O'Connor, T. P. Cytoskeletal events in growth cone steering. *Curr. Opin. Neurobiol.* **4,** 43–48 (1994).

78. Gallo, G. & Letourneau, P. C. Regulation of growth cone actin filaments by guidance cues. *J. Neurobiol.* **58,** 92–102 (2004).

79. Georges, P. C., Hadzimichalis, N. M., Sweet, E. S. & Firestein, B. L. The yin–yang of dendrite morphology: unity of actin and microtubules. *Mol. Neurobiol.* **38,** 270–284 (2008).

80. Polleux, F., Morrow, T. & Ghosh, A. Semaphorin 3A is a chemoattractant for cortical apical dendrites. *Nature* **404,** 567–573 (2000).

81. Hocking, J. C., Hehr, C. L., Bertolesi, G. E., Wu, J. Y. & McFarlane, S. Distinct roles for Robo2 in the regulation of axon and dendrite growth by retinal ganglion cells. *Mech. Dev.* **127,** 36–48 (2010).

82. Dimitrova, S., Reissaus, A. & Tavosanis, G. Slit and Robo regulate dendrite branching and elongation of space-filling neurons in Drosophila. *Dev. Biol.* **324,** 18–30 (2008).

83. Furrer, M.-P., Vasenkova, I., Kamiyama, D., Rosado, Y. & Chiba, A. Slit and Robo control the development of dendrites in Drosophila CNS. *Development* **134,** 3795–3804 (2007).

84. Snider, W. D. Nerve growth factor enhances dendritic arborization of sympathetic ganglion cells in developing mammals. *J. Neurosci.* **8,** 2628–2634 (1988).

85. Ruit, K. G., Osborne, P. A., Schmidt, R. E., Johnson, E. M. & Snider, W. D. Nerve growth factor regulates sympathetic ganglion cell morphology and survival in the adult mouse. *J. Neurosci.* **10,** 2412–2419 (1990).

86. Horch, H. W., Krüttgen, A., Portbury, S. D. & Katz, L. C. Destabilization of cortical dendrites and spines by BDNF. *Neuron* **23,** 353–364 (1999).

87. Baker, R. E., Dijkhuizen, P. A., Van Pelt, J. & Verhaagen, J. Growth of pyramidal, but not non-pyramidal, dendrites in long-term organotypic explants of neonatal rat neocortex chronically exposed to neurotrophin-3. *Eur. J. Neurosci.* **10,** 1037–1044 (1998).

88. Cohen-Cory, S. & Lom, B. Neurotrophic regulation of retinal ganglion cell synaptic connectivity: from axons and dendrites to synapses. *Int. J. Dev. Biol.* **48,** 947–956 (2004).

89. Lom, B. & Cohen-Cory, S. Brain-derived neurotrophic factor differentially regulates retinal ganglion cell dendritic and axonal arborization in vivo. *J. Neurosci.* **19,** 9928–9938 (1999).

90. Volkmar, F. R. & Greenough, W. T. Rearing complexity affects branching of dendrites in the visual cortex of the rat. *Science* **176,** 1445–1447 (1972).

91. Greenough, W. T., Volkmar, F. R. & Juraska, J. M. Effects of rearing complexity on dendritic branching in frontolateral and temporal cortex of the rat. *Exp. Neurol.* **41,** 371–378 (1973).

92. Wiesel, T. N., Hubel, D. H. & others. Effects of visual deprivation on morphology and physiology of cells in the cat's lateral geniculate body. *J Neurophysiol* **26,** 6 (1963).

93. Wiesel, T. N. & Hubel, D. H. Extent of recovery from the effects of visual deprivation in kittens. *J Neurophysiol* **28,** 1060–1072 (1965).

94. Wiesel, T. N. & Hubel, D. H. Comparison of the effects of unilateral and bilateral eye closure on cortical unit responses in kittens. *J Neurophysiol* **28,** 1029–1040 (1965).

95. Hubel, D. H. & Wiesel, T. N. The period of susceptibility to the physiological effects of unilateral eye closure in kittens. *J. Physiol.* **206,** 419 (1970).

96. Hubel, D. H., Wiesel, T. N. & LeVay, S. Plasticity of ocular dominance columns in monkey striate cortex. *Philos. Trans. R. Soc. Lond. B Biol. Sci.* **278,** 377–409 (1977).

97. Smith, Z. D., Gray, L. & Rubel, E. W. Afferent influences on brainstem auditory nuclei of the chicken: n. laminaris dendritic length following monaural conductive hearing loss. *J. Comp. Neurol.* **220,** 199–205 (1983).

98. Lendvai, B., Stern, E. A., Chen, B. & Svoboda, K. Experience-dependent plasticity of dendritic spines in the developing rat barrel cortex in vivo. *Nature* **404,** 876–881 (2000).

99. McBride, T. J., Rodriguez-Contreras, A., Trinh, A., Bailey, R. & DeBello, W. M. Learning drives differential clustering of axodendritic contacts in the barn owl auditory system. *J. Neurosci.* **28,** 6960–6973 (2008).

100. Kalb, R. G. Regulation of motor neuron dendrite growth by NMDA receptor activation. *Development* **120,** 3063–3071 (1994).

101. Vogel, M. W. & Prittie, J. Purkinje cell dendritic arbors in chick embryos following chronic treatment with an N-methyl-D-aspartate receptor antagonist. *J. Neurobiol.* **26,** 537–552 (1995).

102. Portera-Cailliau, C., Pan, D. T. & Yuste, R. Activity-regulated dynamic behavior of early dendritic protrusions: evidence for different types of dendritic filopodia. *J. Neurosci.* **23,** 7129–7142 (2003).

103. Wong, W. T., Faulkner-Jones, B. E., Sanes, J. R. & Wong, R. O. Rapid dendritic remodeling in the developing retina: dependence on neurotransmission and reciprocal regulation by Rac and Rho. *J. Neurosci.* **20,** 5024–5036 (2000).

104. Rajan, I. & Cline, H. T. Glutamate receptor activity is required for normal development of tectal cell dendrites in vivo. *J. Neurosci.* **18,** 7836–7846 (1998).

105. Rajan, I., Witte, S. & Cline, H. T. NMDA receptor activity stabilizes presynaptic retinotectal axons and postsynaptic optic tectal cell dendrites in vivo. *J. Neurobiol.* **38,** 357–368 (1999).

106. Sin, W. C., Haas, K., Ruthazer, E. S. & Cline, H. T. Dendrite growth increased by visual activity requires NMDA receptor and Rho GTPases. *Nature* **419,** 475–480 (2002).

107. McAllister, A. K., Katz, L. C. & Lo, D. C. Neurotrophin regulation of cortical dendritic growth requires activity. *Neuron* **17,** 1057–1064 (1996).

108. Yu, X. & Malenka, R. C. β-catenin is critical for dendritic morphogenesis. *Nat. Neurosci.* **6,** 1169–1177 (2003).

109. Dalva, M. B., Ghosh, A. & Shatz, C. J. Independent control of dendritic and axonal form in the developing lateral geniculate nucleus. *J. Neurosci. Off. J. Soc. Neurosci.* **14,** 3588–3602 (1994).

110. Kossel, A. H., Williams, C. V., Schweizer, M. & Kater, S. B. Afferent innervation influences the development of dendritic branches and spines via both activity-dependent and non-activity-dependent mechanisms. *J. Neurosci.* **17,** 6314–6324 (1997).

111. Armbruster, B. N., Li, X., Pausch, M. H., Herlitze, S. & Roth, B. L. Evolving the lock to fit the key to create a family of G protein-coupled receptors potently activated by an inert ligand. *Proc. Natl. Acad. Sci.* **104,** 5163–5168 (2007).

112. Deisseroth, K. Optogenetics. *Nat. Methods* **8,** 26–29 (2011).

113. Fenno, L., Yizhar, O. & Deisseroth, K. The development and application of optogenetics. *Neuroscience* **34,** 389 (2011).

114. Hua, J. Y., Smear, M. C., Baier, H. & Smith, S. J. Regulation of axon growth in vivo by activity-based competition. *Nature* **434,** 1022–1026 (2005).

115. Dong, W. & Aizenman, C. D. A competition-based mechanism mediates developmental refinement of tectal neuron receptive fields. *J. Neurosci.* **32,** 16872–16879 (2012).

116. Antonini, A., Stryker, M. P. & others. Rapid remodeling of axonal arbors in the visual cortex. *Science* **260,** 1819–1821 (1993).

117. Shatz, C. J. & Stryker, M. P. Ocular dominance in layer IV of the cat's visual cortex and the effects of monocular deprivation. *J. Physiol.* **281,** 267 (1978).

118. Sperry, R. W. Chemoaffinity in the orderly growth of nerve fiber patterns and connections. *Proc. Natl. Acad. Sci.* **50,** 703–710 (1963).

119. Meyer, R. L. Roger Sperry and his chemoaffinity hypothesis. *Neuropsychologia* **36,** 957–980 (1998).

120. Zhang, L. I., Tao, H. W., Holt, C. E., Harris, W. A. & Poo, M. A critical window for cooperation and competition among developing retinotectal synapses. *Nature* **395,** 37–44 (1998).

121. Dong, W. *et al.* Visual avoidance in Xenopus tadpoles is correlated with the maturation of visual responses in the optic tectum. *J. Neurophysiol.* **101,** 803–815 (2009).

122. Cline, H. T. Activity-dependent plasticity in the visual systems of frogs and fish. *Trends Neurosci.* **14,** 104–111 (1991).

123. Tao, H. W. & Poo, M. Activity-dependent matching of excitatory and inhibitory inputs during refinement of visual receptive fields. *Neuron* **45,** 829–836 (2005).

124. Ruthazer, E. S., Akerman, C. J. & Cline, H. T. Control of axon branch dynamics by correlated activity in vivo. *Science* **301,** 66–70 (2003).

125. Ishizawa, Y. Mechanisms of anesthetic actions and the brain. *J. Anesth.* **21,** 187–199 (2007).

126. Haas, K., Sin, W.-C., Javaherian, A., Li, Z. & Cline, H. T. Single-Cell Electroporationfor Gene Transfer In Vivo. *Neuron* **29,** 583–591 (2001).

127. Denk, W., Strickler, J. H., Webb, W. W. & others. Two-photon laser scanning fluorescence microscopy. *Science* **248,** 73–76 (1990).

128. Garaschuk, O. *et al.* Optical monitoring of brain function in vivo: from neurons to networks. *Pflüg. Arch.* **453,** 385–396 (2006).

129. Rathenberg, J., Nevian, T. & Witzemann, V. High-efficiency transfection of individual neurons using modified electrophysiology techniques. *J. Neurosci. Methods* **126,** 91–98 (2003).

130. Kitamura, K., Judkewitz, B., Kano, M., Denk, W. & Häusser, M. Targeted patch-clamp recordings and single-cell electroporation of unlabeled neurons in vivo. *Nat. Methods* **5,** 61–67 (2007).

131. Dunfield, D. & Haas, K. Metaplasticity governs natural experience-driven plasticity of nascent embryonic brain circuits. *Neuron* **64,** 240–250 (2009).

132. Xu, T. *et al.* Rapid formation and selective stabilization of synapses for enduring motor memories. *Nature* **462,** 915–919 (2009).

133. Fu, M., Yu, X., Lu, J. & Zuo, Y. Repetitive motor learning induces coordinated formation of clustered dendritic spines in vivo. *Nature* **483,** 92–95 (2012).

134. Engert, F. & Bonhoeffer, T. Dendritic spine changes associated with hippocampal long-term synaptic plasticity. *Nature* **399,** 66–70 (1999).

135. Maletic-Savatic, M., Malinow, R. & Svoboda, K. Rapid dendritic morphogenesis in CA1 hippocampal dendrites induced by synaptic activity. *Science* **283,** 1923–1927 (1999).

136. Niell, C. M. & Smith, S. J. Functional imaging reveals rapid development of visual response properties in the zebrafish tectum. *Neuron* **45,** 941–951 (2005).

137. Chen, S. X. *et al.* The transcription factor MEF2 directs developmental visually driven functional and structural metaplasticity. *Cell* **151,** 41–55 (2012).

138. Goldin, M., Segal, M. & Avignone, E. Functional Plasticity Triggers Formation and Pruning of Dendritic Spines in Cultured Hippocampal Networks. *J. Neurosci.* **21,** 186–193 (2001).

139. Holtmaat, A., Wilbrecht, L., Knott, G. W., Welker, E. & Svoboda, K. Experience-dependent and cell-type-specific spine growth in the neocortex. *Nature* **441,** 979–983 (2006).

140. Portera-Cailliau, C., Weimer, R. M., De Paola, V., Caroni, P. & Svoboda, K. Diverse modes of axon elaboration in the developing neocortex. *PLoS Biol* **3,** e272 (2005).

141. Changeux, J.-P. & Danchin, A. Selective stabilisation of developing synapses as a mechanism for the specification of neuronal networks. (1976).

142. Cowan, W. M., Fawcett, J. W., O'Leary, D. D. & Stanfield, B. B. Regressive events in neurogenesis. *Science* **225,** 1258–1265 (1984).

143. Podgorski, K., Dunfield, D. & Haas, K. Functional clustering drives encoding improvement in a developing brain network during awake visual learning. *PLoS Biol.* **10,** e1001236 (2012).

144. Chang, F.-L. F. & Greenough, W. T. Transient and enduring morphological correlates of synaptic activity and efficacy change in the rat hippocampal slice. *Brain Res.* **309,** 35–46 (1984).

145. Trommald, M., Hulleberg, G. & Andersen, P. Long-term potentiation is associated with new excitatory spine synapses on rat dentate granule cells. *Learn. Mem.* **3,** 218–228 (1996).

146. Moser, M. B., Trommald, M. & Andersen, P. An increase in dendritic spine density on hippocampal CA1 pyramidal cells following spatial learning in adult rats suggests the formation of new synapses. *Proc. Natl. Acad. Sci.* **91,** 12673–12675 (1994).

147. Kleindienst, T., Winnubst, J., Roth-Alpermann, C., Bonhoeffer, T. & Lohmann, C. Activity-dependent clustering of functional synaptic inputs on developing hippocampal dendrites. *Neuron* **72,** 1012–1024 (2011).

148. Harvey, C. D. & Svoboda, K. Locally dynamic synaptic learning rules in pyramidal neuron dendrites. *Nature* **450,** 1195–1200 (2007).

149. Harvey, C. D., Yasuda, R., Zhong, H. & Svoboda, K. The spread of Ras activity triggered by activation of a single dendritic spine. *Science* **321,** 136–140 (2008).

150. Kwon, H.-B. & Sabatini, B. L. Glutamate induces de novo growth of functional spines in developing cortex. *Nature* **474,** 100–104 (2011).

151. Nikonenko, I., Jourdain, P. & Muller, D. Presynaptic Remodeling Contributes to Activity-Dependent Synaptogenesis. *J. Neurosci.* **23,** 8498–8505 (2003).

152. Ninan, I., Liu, S., Rabinowitz, D. & Arancio, O. Early presynaptic changes during plasticity in cultured hippocampal neurons. *EMBO J.* **25,** 4361–4371 (2006).

153. Medvedev, N. I. *et al.* Multiple spine boutons are formed after long-lasting LTP in the awake rat. *Brain Struct. Funct.* **219,** 407–414 (2012).

154. Wolff, J. R., Joó, F. & Dames, W. Plasticity in dendrites shown by continuous GABA administration in superior cervical ganglion of adult rat. *Nature* **274,** 72–74 (1978).

155. Dudek, S. M. & Bear, M. F. Homosynaptic long-term depression in area CA1 of hippocampus and effects of N-methyl-D-aspartate receptor blockade. *Proc. Natl. Acad. Sci.* **89,** 4363–4367 (1992).

156. Mulkey, R. M. & Malenka, R. C. Mechanisms underlying induction of homosynaptic long-term depression in area CA1 of the hippocampus. *Neuron* **9,** 967–975 (1992).

157. Iyer, V., Hoogland, T. M. & Saggau, P. Fast functional imaging of single neurons using random-access multiphoton (RAMP) microscopy. *J. Neurophysiol.* **95,** 535–545 (2006).

158. Reddy, G. D., Kelleher, K., Fink, R. & Saggau, P. Three-dimensional random access multiphoton microscopy for functional imaging of neuronal activity. *Nat. Neurosci.* **11,** 713–720 (2008).

159. Chen, T.-W. *et al.* Ultrasensitive fluorescent proteins for imaging neuronal activity. *Nature* **499,** 295–300 (2013).

160. Gaudilliere, B., Konishi, Y., de la Iglesia, N., Yao, G. & Bonni, A. A CaMKII-NeuroD signaling pathway specifies dendritic morphogenesis. *Neuron* **41,** 229–241 (2004).

161. Zhai, S., Ark, E. D., Parra-Bueno, P. & Yasuda, R. Long-distance integration of nuclear ERK signaling triggered by activation of a few dendritic spines. *Science* **342,** 1107–1111 (2013).

162. Kitamura, K., Judkewitz, B., Kano, M., Denk, W. & Häusser, M. Targeted patch-clamp recordings and single-cell electroporation of unlabeled neurons in vivo. *Nat. Methods* **5,** 61–67 (2008).

163. Judkewitz, B., Rizzi, M., Kitamura, K. & Häusser, M. Targeted single-cell electroporation of mammalian neurons in vivo. *Nat. Protoc.* **4,** 862–869 (2009).